Coupled tectonic and sedimentary evolution in asymmetric extensional basins: The Konjic Basin in the Dinaride Lakes System of Bosnia and Herzegovina

Abstract

The evolution of sedimentary basins can be derived by studying the link between fault kinematics and sedimentation. Sedimentation in asymmetric extensional basins is controlled by the accommodation space formed in the hanging wall of normal faults and by the variability of a source area controlled by their coeval footwall exhumation. One very good place to study this relationship is the External Dinarides of Bosnia and Herzegovina, where a large number of Miocene asymmetric extensional basins have formed by the reactivation of an inherited Cretaceous – Eocene nappe stack. These Early-Middle Miocene basins formed as endemic and endorheic lakes and are generally known as the Dinaride Lakes System (DLS). In the DLS, one very good place to analyse the link between the activation of normal faults and the associated sedimentation is the Konjic Basin in the central part of the External Dinarides, which contains continuous and well-preserved outcrops exposing both the normal faults and their associated sedimentary facies. In this basin, we have performed a detailed kinematic and sedimentological mapping that allowed a correlation between normal faulting events and the associated depositional facies. The results show that normal faults have been created in response to a first extensional stage oriented NE-SW that was followed by a second extensional stage oriented NNE-SSW. Sedimentological field observations have allowed the definition of facies units that were subsequently grouped in facies associations. These facies association are characterized by fining and coarsening upward patterns, interpreted to be formed in response to second-order progradation-retrogradation (P-R) cycles. The correlation with the moments of normal fault activation shows a causal link between faulting and slope instability. Activation of normal faults triggers avalanching of coarse material towards the deeper parts of the basin, resulting in alternating successions of alluvial-fluvial and deltaic deposits. These sediments record downslope flow transformations from debris flow to subaqueous turbidity currents, which create the observed fining and coarsening upward patterns. This study indicated at least six tectonically induced second-order P-R cycles that formed in response to the activation of clear sets of normal faults. Grouping the second-order P-R cycles allows the definition of a lower order P-R cycle, associated with the opening and subsequent filling-up of the entire basin. Our results indicate that the Middle Miocene basin evolution of the Konjic Basin was controlled by large-scale exhumation in the footwall. Previous studies on DLS basins in the External Dinarides show similar characteristics for this Early-Middle Miocene period of extension, generally thought to be related to the back-arc opening of the Pannonian Basin. In these DLS basins footwall exhumation is created by extension and is accommodated by detachments branching into inherited weak zones. The footwall uplift that controlled the sedimentation of the Konjic Basin development is accommodated by an in opposite directed normal detachment when compared with the larger scale Buscovača detachment that controls the evolution of the larger Sarajevo-Zenica Basin situated northwards. On the overall, our research contributes to a better understanding of the mechanisms controlling the sedimentary response to extensional basin formation and the genetic link with footwall exhumation in asymmetric intra-montane basins.

Jacob M. Dekker 3820866

Supervision: Prof. Dr. L.C. Matenco & Dr. N. Andrić
Utrecht University, Department of Earth Sciences

J.M.Dekker@students.uu.nl & Dekker.Jacob.M@gmail.com
1st submitted manuscript 28-03-2018
Final manuscript 14-11-2018

Universiteit Utrecht

Key words: Early-Middle Miocene extension, Dinarides lakes sediments, asymmetric extensional basins, progradation-retrogradation cycles, footwall uplift, sedimentary evolution

ABSTRACT 1

1. Introduction **3**

2. The Konjic Basin in the context of the Dinarides **4**

3. Methodology **7**

4. Results **9**
4.1. Basin Kinematics 9
4.1.1. Large scale extension 9
4.2. Sedimentary environments during the Middle Miocene extension 15
4.2.1. Facies associations 15
4.2.2. P-R cycles 21

5. Link between Middle Miocene extension and evolution of facies associations **24**
5.1. Second order P-R cycles 24
5.2. First-order P-R cycles 27
5.2.1. First-order retrogradation 27
5.2.2. First order progradation 30
5.2.3. Cross-sectional model 32

6. Tectonic and sedimentary evolution of the Konjic Basin in context of the Dinarides **34**

7. Conclusions **36**

8. Acknowledgements **36**

9. References **37**

Appendix A **40**

1. Introduction

The architecture of extensional intra-montane sedimentary basins reflects the interplay between available accommodation space and sediment supply (e.g. Schlager, 1993; Gawthorpe and Leeder, 2000). Sedimentation rates, spatial and temporal facies variability is not only controlled by tectonic and climate conditions, but also by the inherited orogenic structure (e.g. Bochas et al., 2000). In the Mediterranean region many intra-montane basins formed during an extensional episode that followed the main orogenic build-up. The extensional episode is often characterized by reactivation of former suture zones, nappe contacts or thrusts as low-angle normal faults or detachments. During the reactivation of pre-existing structural fabrics, the formation of asymmetric extensional basins is favoured in the hanging wall of previous nappe contacts reactivated as detachments associated with exhumation of deeply buried tectonics units in their footwall (Brun and Faccenna, 2008). The formation of extensional detachments and normal faults creates core-complexes as well as sedimentary extensional basins and plays an important control on the formation of accommodation space and sediment supply (Jolivet and Faccenna, 2000). In such basins, faulting dynamics, such as migration and slip rates copntrois the basin subsidence and coeval footwall exhumation. Regions with a thickened crust, like orogenic build-ups, experience upward movement of the footwall during extension which controls the sedimentation in asymmetric intra-montane basins (Bertotti et al., 2000). Sediments in these basins record the response to fault activity and or perturbation of its slip rates (Andrić et al., 2018). Despite this advance understanding, the relation between extension and sedimentation in asymmetric basins within an inherited orogenic setting is still not fully understood.

The Dinarides are a good place to study the relationship between nappe stacking and reactivation by detachments and formation of asymmetric extensional basins. Previous studies have shown that these basins in the External Dinarides have formed in response to a stage of NE-SW Miocene extension followed by still ongoing N-S shortening (Hrvatovic, 2005; van Unen et al., 2018). In this area, such basins formed as a consequence of the Early-Middle Miocene re-activation of inherited thrusts, nappe contacts or major suture zones (Ustaszewski et al., 2014; Balasz et al., 2016). These extensional basins developed throughout the Early-Middle Miocene as isolated lakes and are generally known as the Dinaride Lakes System (DLS) (Harzhauser and Mandic; 2008; de Leeuw et al., 2011; Mandic et al., 2011) (fig. 1a; fig. 1b). Sedimentary deposition in DLS basins in the Dinarides is mainly controlled by tectonically induced subsidence and footwall uplift. The Miocene basins situated at the northern boundary of the Dinarides Mountains have been interpreted as a consequence of the back-arc opening of the Pannonian Basin in response to the roll-back of the Carpathians and Dinarides slabs (Matenco and Radivojevic, 2012). The endorheic character of Early-Middle Miocene DLS basins allows a direct correlation between sediment input and footwall erosion. However, the relation between extension and sedimentation is influenced by coeval Middle Miocene Climatic Optimum (MCO) (Sant et al., 2018). The MCO induced an imbalance in precipitation and evaporation rates which presumably disturbed the sedimentary record in DLS basins (Mandic, et al., 2011). However, one DLS basins where the tectonic signal can be correlated with sedimentation in an extensional asymmetric basin due to its well-exposed continuous outcrops, is the Konjic Basin situated in the central-southern part of the Dinarides (Fig. 1). It formed on the SW margin of the Pre-Karst unit, in close proximity of an inherited contact between the Pre-Karst and the High-Karst nappes (Hrvatovic, 2006). Many DLS basins such as the neighbouring Sarajevo-Zenica Basin are controlled by a detachment that reactivates a nappe contact and accommodates extensive footwall uplift (Andrić et al., 2017). It is unknown whether this mechanism is applicable to the Konjic Basin. Alluvial, fluvial, turbiditic and lacustrine sediments have been deposited in the Konjic Basin as the sedimentary response to its Middle Miocene evolution, extensional and/or climatic induced. The detailed sedimentary and tectonic evolution is still unknown for the Konjic and many other Miocene DLS basins (Andrić et al., 2017).

We have performed a field kinematic and sedimentological analysis in the Konjic basin in order to correlate the sedimentary record to the formation and evolution of the controlling normal faults and the associated moments of slope instability. The field study has allowed the definition of facies units, facies associations (depositional environments) and finally system tracts. The model of the Konjic Basin is compared to previous results obtained in neighbouring areas (Hrvatovic, 2006; Andrić et al., 2017; van Unen et al,. 2018; and references therein). The correlation between the sedimentological analysis and the kinematics of normal faults has allowed the definition of a novel and detailed Early-Middle Miocene extensional model for the Konjic Basin that is coherent with the kinematics and sedimentology of the External Dinarides in general. Therefore, this study provides new insights into the understanding of the evolution of asymmetric basin within an inherited structural grain and into the evolution of the External Dinarides in general.

2. The Konjic Basin in the context of the Dinarides

The Dinarides are part of the Alpine-Himalayan orogenic system that formed as a complex fold, thrust and imbricate belt in response to the Middle Triassic opening and the Middle Jurassic – Paleogene closure of the Neotethys Ocean and continental collision between Europe- and Adriatic-derived continental units (Schmid et al., 2008; Pamic et al, 2002; Pamic et al., 1998). Cretaceous-Oligocene successive orogenic shortening events created SW-vergent thrusting and the formation of a nappe stack structure that is generally subdivided into the Internal and External Dinarides (fig. 1a) (Schmid et al., 2008; Ustaszewski et al, 2014; Andrić et al., 2017). The Internal Dinarides nappes are composed of pre-Mesozoic basement, Mesozoic sediments of the former continental passive margin, ophiolites and accretionary wedges that are subsequently stacked during Cretaceous to Paleogene times (Schmid et al., 2008). The Internal Dinarides are made up of a sequence of thrusted units that are, from NE to SW in a highest to lowest structural position, Jadar-Kopaonik, Drina-Ivanjica, East Bosnian-Durmitor and Pre-Karst units (fig. 1a). The same SW-vergent thrusting affected also the External Dinarides by stacking three more nappes in a lower structural position with respect to more internal units by following the same thrusting vergence towards the SW. In the same structural position these units are the High-Karst, Budva-Cukali and Dalmatian units, the latter being thrusted over the undeformed Adriatic foreland (fig. 1a). These external nappes are composed of Adriatic Mesozoic to Paleogene shallow marine carbonate platforms, syn-contractional sediments and locally contain Paleozoic basement (Ustaszewski et al, 2014).

The External Dinarides are affected by an Early – Middle Miocene period of extension (de Leeuw et al., 2012). This extension is commonly attributed to the opening of the extensional Pannonian back-arc basin (starting ~20 My ago) controlled by the roll-back of the Carpathians and Dinarides slabs, which resulted in extension and the reactivation of nappe stack contacts in the Dinarides as extensional detachments (Matenco and Radivojevic, 2012). In the course of extension, deeply buried tectonic units are exhumed by footwall uplift in the Internal Dinarides (Ustaszewski et al., 2014). The neighbouring Sarajevo-Zenica Basin indicated up to ~8km of exhumation (Andrić et al., 2017)

Miocene extension favoured the formation of the Dinaride Lakes System (DLS) (Harzhauser and Mandic, 2008; De Leeuw, 2011). The sedimentary stratigraphy in these lakes provides excellent insight into the paleoenvironmental and paleobiogeographic evolution of the Dinarides due to their endemic and endorheic character. Most of the lakes developed isolated, but some developed together as a single lake and were disconnected in a later stage (Mandic et al, 2011; de Leeuw, et al., 2011) (fig. 1b). The basin formation coincides with the Miocene Climatic Optimum, based on ages of sediments in DLS basins Sinj, Livno and Gacko on the High-Karst Nappe (fig. 1b) (de Leeuw, 2011). The formation of these Early-Middle Miocene basins has been interpreted in various ways, such as an effect of the

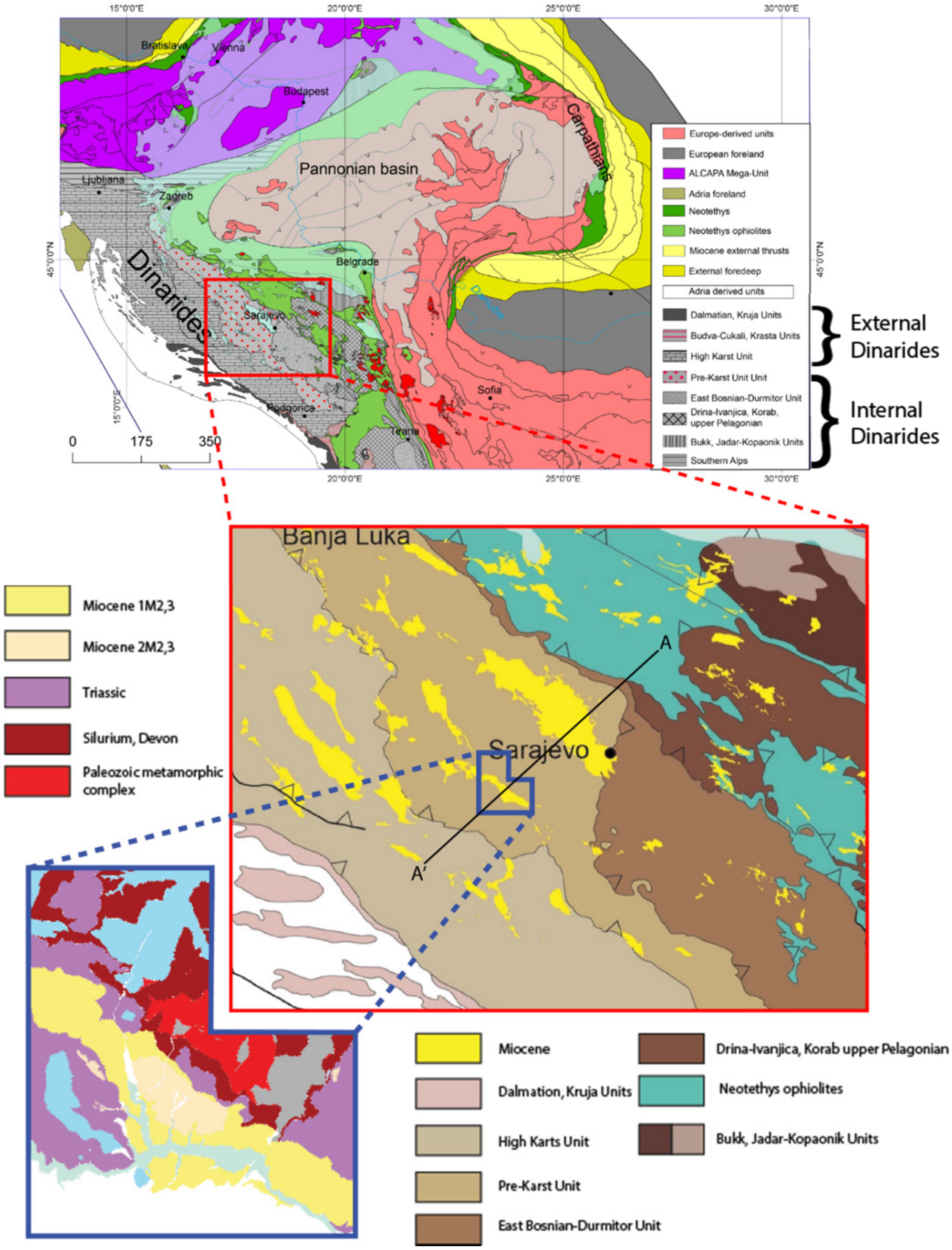

Figure 1: a) Geological map of the Alps-Carpathian-Dinaride system from Andrić et al. (2017). See text for more detailed description of the units building-up the internal and external Dinarides. b) Geological setting of present-day remains of intra-montane (Dinaride Lakes System) basins. Map illustrating the nappe contacts and plate boundaries between different units.

A-A' corresponds to the transect from figure 24. Blue polygon outlines the Konjic Basin. For more detail on the Konjic Basin, see figure c. c) Simplified geological map of the Konjic Basin and surrounding tectonic units.

Adriatic microplate rotation and its indentation into Eurasia. This rotation and indentation created shortening of the Variscan and Alpine tectonostratigraphic units leading to a transpressional phase that is characterized by strong strike-slip (mainly dextral) faulting, producing NW-ESE orientated depressions (Hrvatovic, 2005). An alternative hypothesis takes into account the opening of the Pannonian Basin and coeval Miocene Climatic Optimum, which created favourable climatic conditions (De Leeuw et al., 2011).

One of these under-explored DLS basins is the Konjic Basin which is situated in the Pre-Karst unit at the margin of the inherited nappe contact between the Pre-Karst and the High-Karst unit formed during Eocene thrusting (fig. 1b) (van Unen et al., 2018). The NW margin of this basin consists of Mid-Bosnian Schist Mountains complex (MBSMs) that is a build-up of Variscan metasediments, metavolcanics, post-Variscan formations and Mesozoic cover. The post-Variscan formations are unconformably overlain by a Permian-Mesozoic cover that is composed of Permian - Lower Triassic evaporites and clastics, and Middle Triassic – Cretaceous carbonate sediments deposited over the passive Adriatic continental margin (Pamic et al., 2004; Hrvatovic, 2005). The Vrbas fault delineates the contact between the MBSMs and the basin(fig. 1).

Similar sedimentary records in nearby basins indicate that the Miocene lake covered a larger area extending from the Konjic Basin up to the Repovac and Prozor basins and were subsequently disconnected later by a contractional deformation phase (Sofilj and Zivanovic, 1971). The sedimentary record in these basins consists of continental deposits of previously interpreted Middle Miocene age. Three continental units are distinguished (fig. 2) (Sofilj and Zivanovic, 1971): (1) the oldest unit (Lower Middle Miocene, $^{1}M_{2,3}$) is comprised of conglomerates, sandstones and breccias in the base. (2) The second unit (Mid-Middle Miocene, $^{2}M_{2,3}$) of marlstones and marly limestones with coal, and (3) the third unit (Upper Middle Miocene, $^{3}M_{2,3}$) is composed of conglomerates and sandstones. The $^{3}M_{2,3}$ unit is missing in the Konjic Basin (fig. 3).

The oldest unit recognized in the Konjic Basin is unit $^{1}M_{2,3}$ (fig. 2) which is comprised of well-cemented conglomerates, breccias and sandstones that consist almost exclusively of grey-green Palaeozoic schists. The fragments are of variable sizes and cemented with a clayey and iron-rich matrix. These deposits occur on both basin margins and are built mainly from the pebbles of Palaeozoic rocks.

Laterally and vertically $^{1}M_{2,3}$ grades into unit $^{2}M_{2,3}$ (fig. 2). This unit is formed in a marshy environment (coal layers) but also in profundal lake facies indicated by marly limestones which are intercalated with clays. The age determined on the mammalian fauna found in coal layers in the Prozor basin is confirmed by floristic age determination of marlstones from Repovec (Malez and Slišković, 1976) and correspond to a Middle and Upper Miocene age. The thickness of these sediments ranges between 150 and 400 m.

Unit $^{3}M_{2,3}$ (fig. 2) is made up by well-cemented conglomerates, build-up of material of the Palaeozoic and sandstones covered with approximately 10 cm thick sandy brooms. Marlstone sediments and coal deposits are found on top.

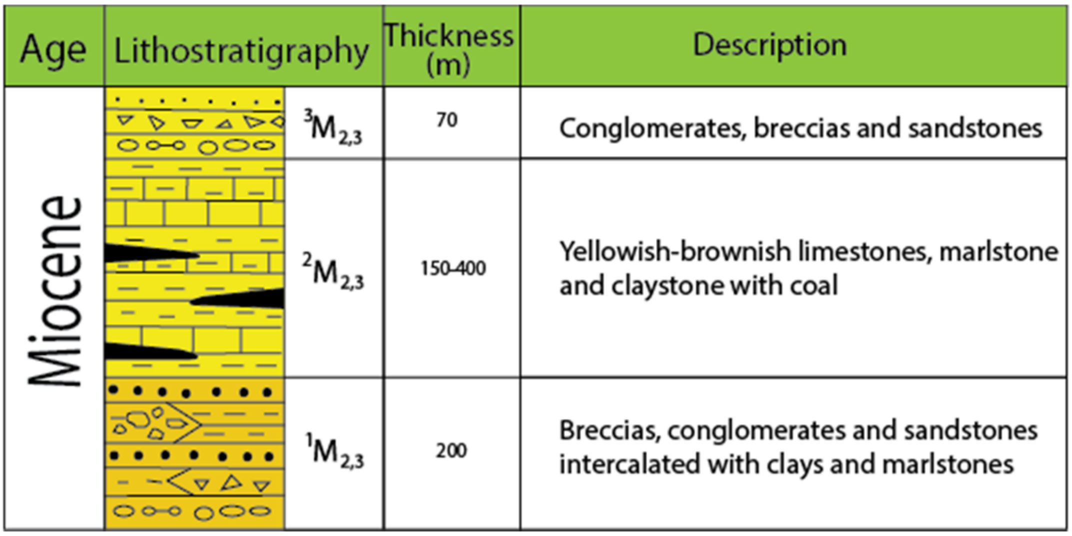

Figure 2: Tectonostratigraphic column of the Konjic-Repovac and Prozor basin. Ages, lithostratigraphy, thickness and description is modified after (Sofilj and Zivanovic, 1971).

3. Methodology

Very well exposed laterally continuous outcrops in the Konjic Basin allowed mapping of sedimentary facies and fault kinematics. Mapping mainly followed sections in road-cuts surrounding the present-day lake and isolated outcrops throughout the Konjic Basin (fig. 3). Faults, bedding and shear sense indicators including Riedel shears, conjugate faults, slickensides and fault-drag structures were measured. Relative timing of deformation is derived using cross-cut relations, stratigraphic relations and bedding measurements. Syn-kinematic faults are often observed with a clastic wedge in the hanging wall (fig. 6a). Distinction between antithetic and synthetic wedges is based on the direction of normal faulting and the orientation of deposition (Andrić et al., 2018), i.e. either sediments are deposited over the fault scarp or deposited over the rotated hanging wall block. Multiple tectonic phases are identified based on stratigraphic age, type of deformation and calculated stress orientation. Faults cross-cutting the entire outcrop and faults that do not show a clastic wedge, indicative for the timing of faulting, are disregarded for determination of the chronology of faulting events within the basin. However, in a later stage, these faults are grouped into one of the indicated faulting phases generally based on the stratigraphy and fault kinematics (orientation, shear sense and geometry) in order to calculate cumulative offsets per tectonic phase.

Syn-kinematic faults and their shear senses, and clastic wedges subsequently tilted by later tectonic events are restored using the position of overlying strata. Based on facies associations, the original depositional angle is restored to a maximum inclination up to 15 degrees in the case of the delta slope deposits.

Sedimentological data acquisition is primarily based on facies units (table 1) logging across the basin. During these logging surveys, special attention was paid to the lateral and vertical evolution of sedimentary strata. Geometry, sedimentary structure, grain, colour, thickness, fossil content and boundary geometries are used to determine the facies units (table 1). Subsequently, the facies units are gathered into facies associations (fig. 9; fig. 10) and finally, the facies associations are grouped into genetic units which are analysed in the context of progradation and retrogradation depositional trends.

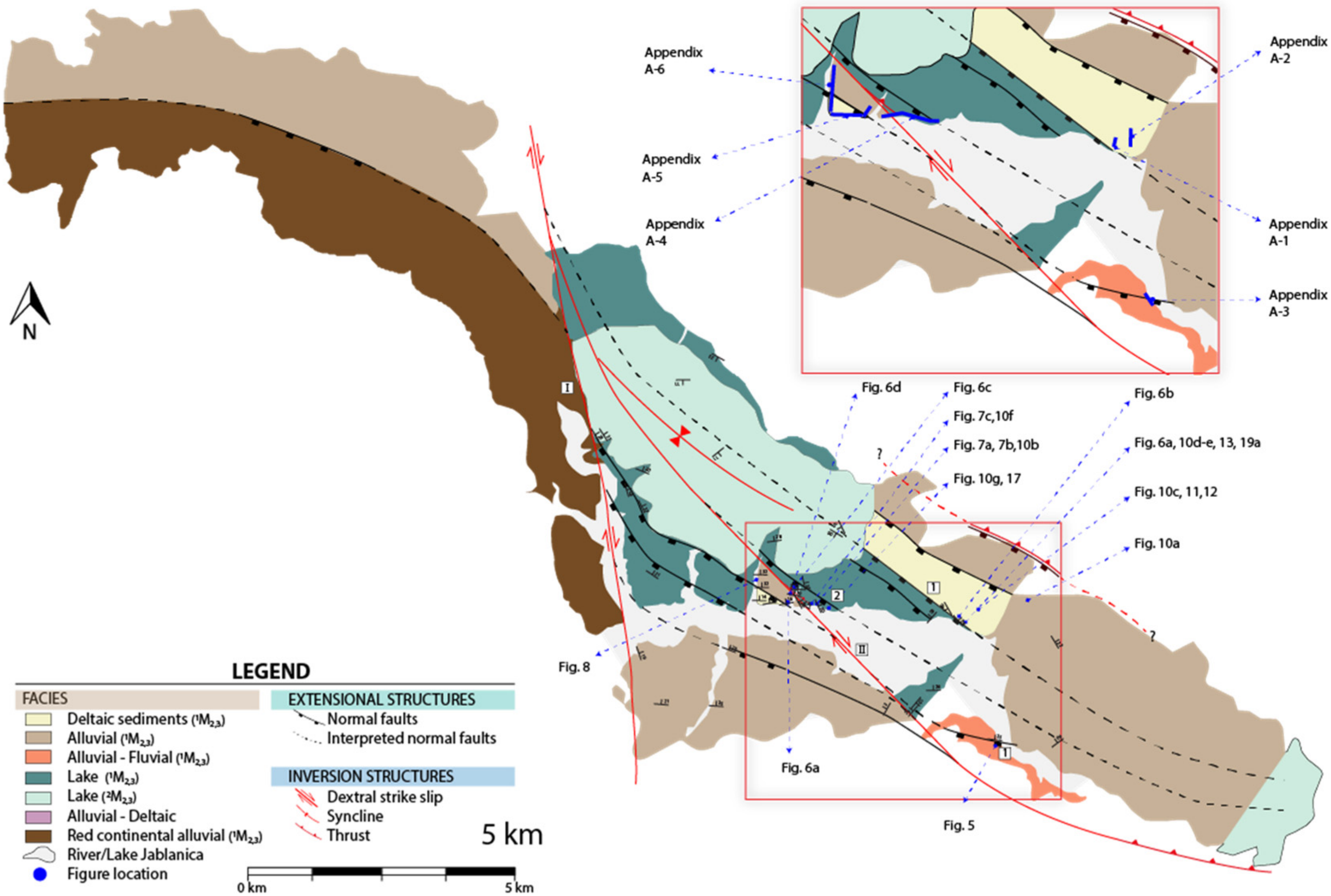

Figure 3: Simplified kinematic and sedimentological map of the Konjic basin after Hesselberth, 2018 and the results of this study. Illustrating structures active during different deformation events. The sedimentary units associated with $^{1}M_{2,3}$ are deposited as a response to the extensional phase. The black lines and the black dotted lines are also associated with the extensional phase. The red lines are associated with a latter inversion. Blue dots indicate the location of outcrops in figure 5, 6, 7, 8, 10, 11, 12, 13, 17 and 19 and blue solid lines the logging tracks corresponding to Appendix A.

4. Results

4.1. Basin Kinematics

Two deformational phases are identified within the basin; (1) an overall extensional phase characterized by large-offset NW-SE oriented normal faults and (2) one other subsequent deformation phase characterized by a stress regime with N-S oriented compression. During the latter phase, the older NW-SE oriented normal faults were affected by dextral strike-slip, reverse and thrusts faults showing N-S oriented shortening. Our study focuses on the Early-Middle Miocene NE-SW oriented extensional phase, which occurred coevally with the formation of the Dinaride Lakes System (DLS) and the evolution of the Konjic Basin. The effect that inherited structures, especially ongoing deformation, have on the Middle Miocene extensional geometries and structures is in particular considered.

4.1.1. Large scale extension

The first deformational phase observed in the Konjic Basin is extensional and characterized by normal faults with varying offsets between 0,1 and 10 meters. The overall extensional direction is NE-SW with dominant top to SW sense of movement (fig. 4). In more detail, the extension shows a change in direction upwards in the stratigraphy, from NNE-SSW to NE-SW and eventually NW-SE (fig. 4). Many of the faults observed in the studied area are syn-depositional, which means that they are associated with clastic wedges in the hanging wall and/or sealed by finer material (fig. 5; fig. 6; fig. 7). Stratigraphic correlation of syn-kinematic structures allowed the subdivision of 3 phases of normal fault activity during the Middle Miocene extensional phase. Cumulative offset of all normal faults indicated in the Konjic Basin is estimated to be 150 meters, which is incongruent with the earlier described lithostratigraphic thickness of 350-600 meter (Sofiji and Zivanovic, 1975) (fig. 2). This inconsistency can be explained by many explanations such as poor exposition of faults and syn-kinematic wedges, simple lake level rise by favourable conditions or basin subsidence. Therefore, it is presumed that cumulative offset is higher than 150 m. Nevertheless, the number and average offset of observed faults reveals that the cumulative offset of the second extensional phase is the largest (~85 m), respectively followed by the first (~45 m) and the third phase (~20 m).

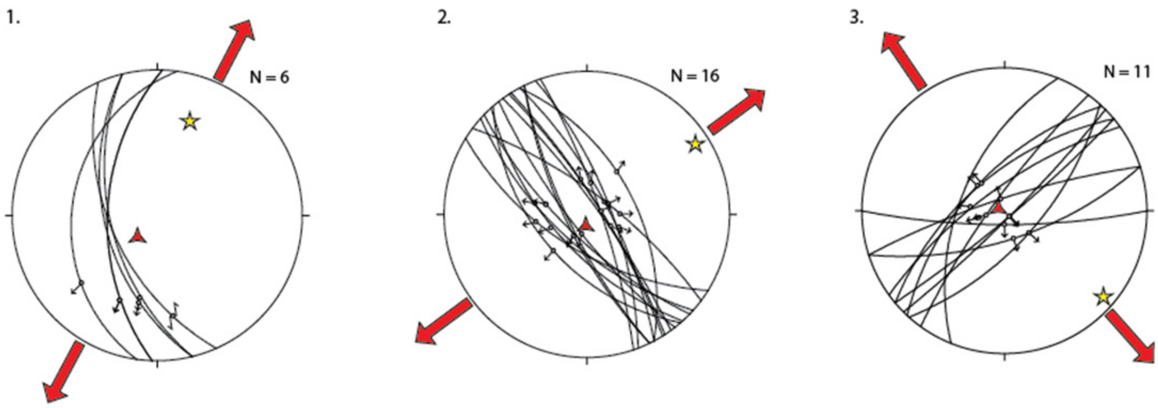

Figure 4: Extensional Middle Miocene kinematic phases recorded in the Konjic Basin. Red triangle and yellow star represent orientation of the stressfieldσ1 and σ3 i.e. respectively σ1 and σ3. 1) The first phase shows oblique NNE-SSW extension; 2) The abundant recorded second phase clearly shows NE-SW extension; 3) The youngest extensional phase exhibits NW-SE extension. Note: The data from the youngest phase (3), indicating NW-SE extension, is most likely influenced by latter large strike-slip faulting affecting the extensional orientation.

4.1.1.1 The first phase of normal fault activity

The first phase of extension in the Konjic Basin is characterized by normal faults with varying offsets between 10m and 0.2m with a NNE-SSW extensional direction that cross-cut alluvial and deltaic deposits which are associated with the oldest basin unit $^{1}M_{2,3}$ (Sofilj and Zivanovic, 1971) (fig. 2). Large faults (~10 m) have slightly listric geometry and generally show top to SSW direction with an oblique slip component of approximately 20° (fig. 4.1 & fig. 6a). Conglomeratic antithetic wedges formed against the fault scarp illustrate that created accommodation space is immediately filled-up by more immature sediments (fig. 6a). Drag structures in the footwall clearly indicate sense of movements (fig. 6a). Syn-kinematic wedges indicate that the rate of filling-up of the created accommodation space is high (fig. 6a). Faults that focus flow, creating an erosional surface at the base of the syn-kinematic wedge are located In the southern part of the basin (fig. 5). Smaller faults with varying offsets between 1 and 0,2 meter have a dominantly planar geometry (fig. 6b). Although these faults often lack a syn-kinematic wedge, relative timing of faulting could still be constructed by comparing the offsets at the bottom with the offsets at the top of the exposed faults. Field examples (e.g. figure 6b) demonstrates that deposition took place simultaneously with normal faulting since the offset at the top of the fault is smaller than at the bottom. The same fault is sealed by a medium sand-sized layer, emphasizing the syn-kinematic character of these faults.

Figure 5: Field example: Flow focused in the small depo-center created by the normal fault. The channel has incised in the underlying strata and against the fault scarp. Green solid line indicates an erosional surface, red solid line indicates a normal fault and the black solid lines indicate bedding planes. See figure 3 for the location.

4.1.1.2 The second phase of normal fault activity

The second phase is characterized by NE-SW extensional direction normal faults (fig 4.2) that have medium size offsets (>3 m) with a top to the SW sense of shear (fig 6d). Almost all faults result in 70°

dipping normal faults after back-tilting (fig 4.2 and 6d). The smaller faults (<1 m) tend to be without a clear sense of shear?. They are planar and show signs of refraction while cutting through layers with varying competence (fig. 4.2; fig. 7c). Faults with a syn-kinematic wedge are not as common as within the first phase of extension. In this case, slumps and relatively finer layers overlying faults allow for a chronological determination of this faulting phase (fig. 7). Unexposed faults only exhibiting the syn-kinematic wedge also provide indirect information on the faulting regime (see fig. 7a-b captions for a detailed description). The wedge and its internal geometry indicate that the structure is induced by a normal fault.

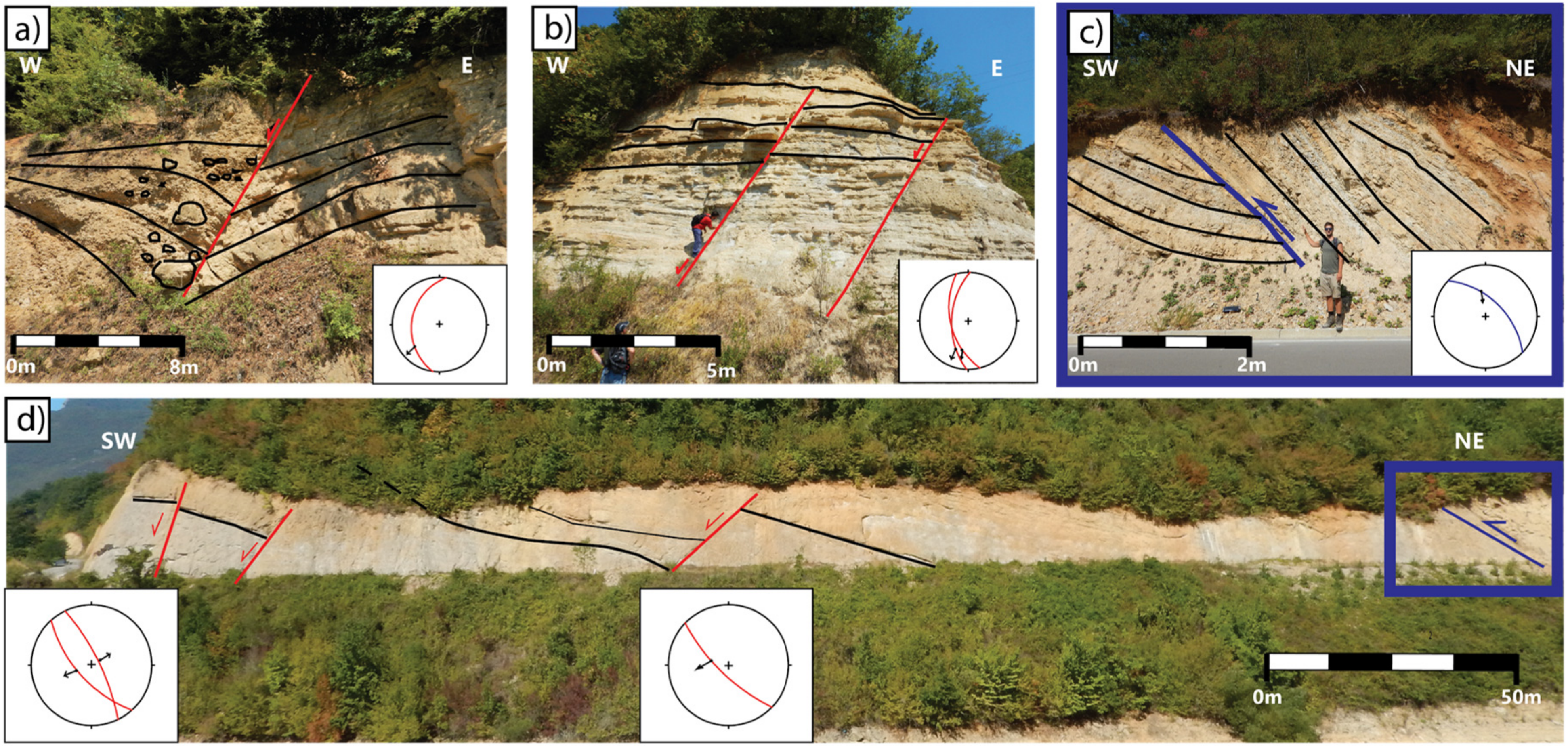

Figure 6: Field examples: Syn- and post-depositional normal faults during the Middle Miocene. a) A conglomeratic antithetic wedge is formed left to a syn-kinematic normal fault associated with the first phase of Middle Miocene extension (10 meter offset). The wedge is more immature than the underlying and adjacent sediments in the footwall. b) Two normal faults in lobe and channelized sequence of silts, sandstones and conglomerates associated with the first phase of extension. Normal fault I is syn-kinematic, the top of the fault is overlain by sandy sediments. Normal fault II on the right is cross-cutting the entire section. Accumulative offset of both faults is approximately 4 meter and is associated with the first phase of extension. Note the decreasing offsets from bottom to top along the fault plane.. c) A field example of a thrust fault cross-cutting the entire turbiditic sequence. This fault is associated with the younger N-S contraction d) Panorama showing the thrust fault of fig. 6c on the right. On the left and in the middle of the panorama three normal faults with accumulative offset of ~18 meter affiliated with the second extensional phase. Note that the stereonets represent the restored fault kinematics. See figure 3 for the locations.

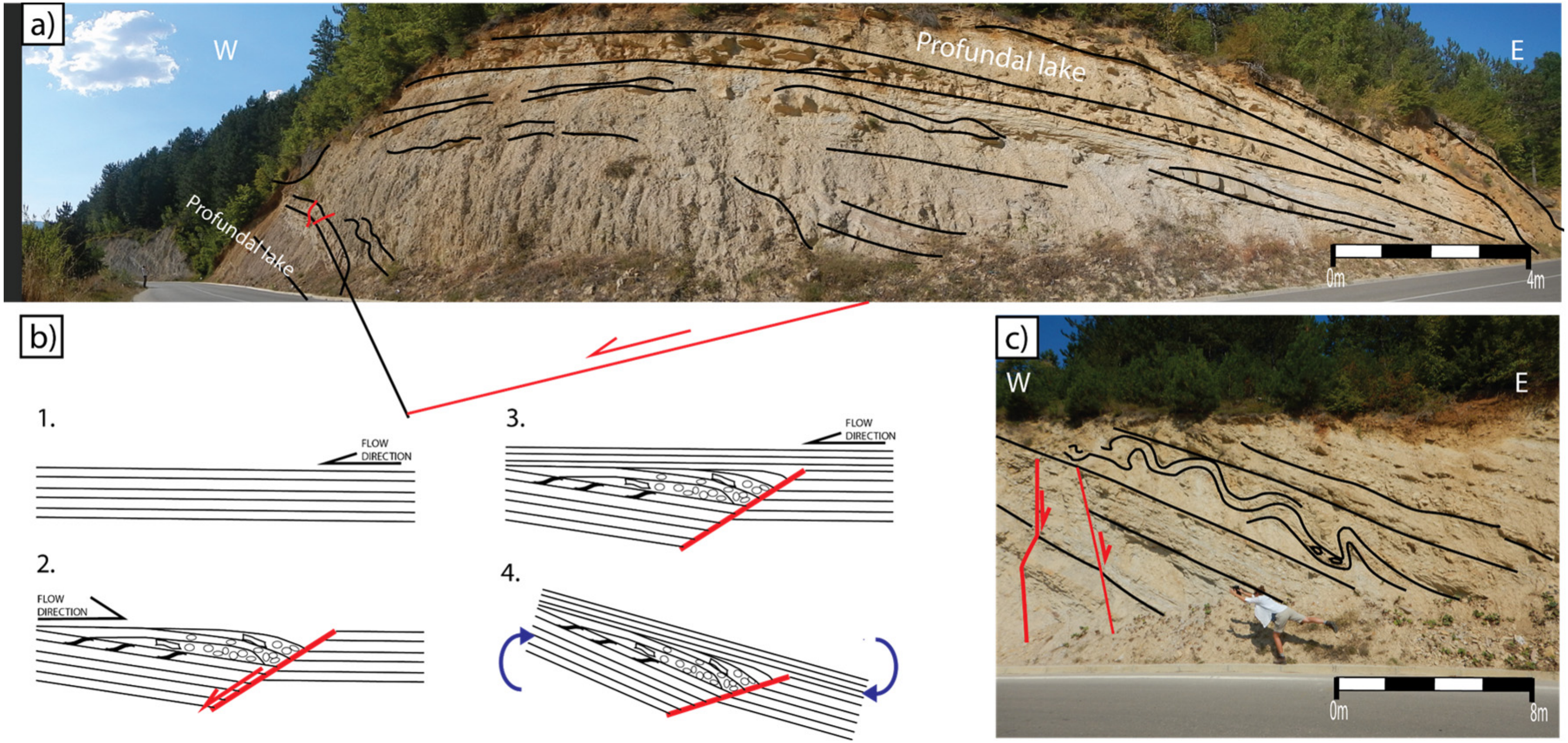

Figure 7: Illustrating the effect of normal fault activity on prodelta facies associations. a) Field example showing PL (Profundal lake) facies association overlies wedge geometry of PD1,2 (prodelta). The wedge contains shear structures at the base and massive rip-ups of claystone. b) A four step illustration explaining the massive wedge geometry of figure 7a. 1. Normal deposition of distal profundal lake with limited prodelta deposits with flow direction towards the SW. 2. Normal faulting created a tilted half-graben structure. The faulting event, disturbed the sediments on the slope, and coarse material is shed downslope into the fault created space. A high energy cohesion flow created shear structures and rip-ups while it moved downslope to fill the hole. The top of the fault is eroded and the accommodation space is filled up. 3. Profundal lake sediments are deposited after the faulting event. 4. Subsequent tilting of the sediments due to the still present-day active N-S phase of contraction. c) Slump overlying two syn-kinematic normal faults. Differences in competence results in refraction of the fault. It becomes steeper in more competent material. Both faults do not cross-cut the slumped package. See figure 3 for the locations.

4.1.1.3 The third phase of normal fault activity

The third phase is characterized by a large amount of normal faults with small varying offsets from 0.1 to 1 meter and a NW-SE extensional direction without a dominant sense of shear (fig. 4.3). The faults in this phase are bounded to a small area, composed of conglomerates with high competence. The normal faults appear to have a 80-90^{o} angular difference with their conjugate faults. The conglomeratic and high competence character presumable influence the formation of typical 60^{o} conjugate fault sets. Cross-cut relations between the two planes indicate that there is not an extra deformation phase. Further investigation of surrounding kinematic features revealed the proximity to a younger strike-slip fault (fig. 3). The structural map of the Konjic Basin indicates that these normal faults are presumably rotated by this younger strike-slip zone. This has led to the conclusion that these faults are influenced in such a manner that back-tilting only restores the original inclination and not the dip-direction.

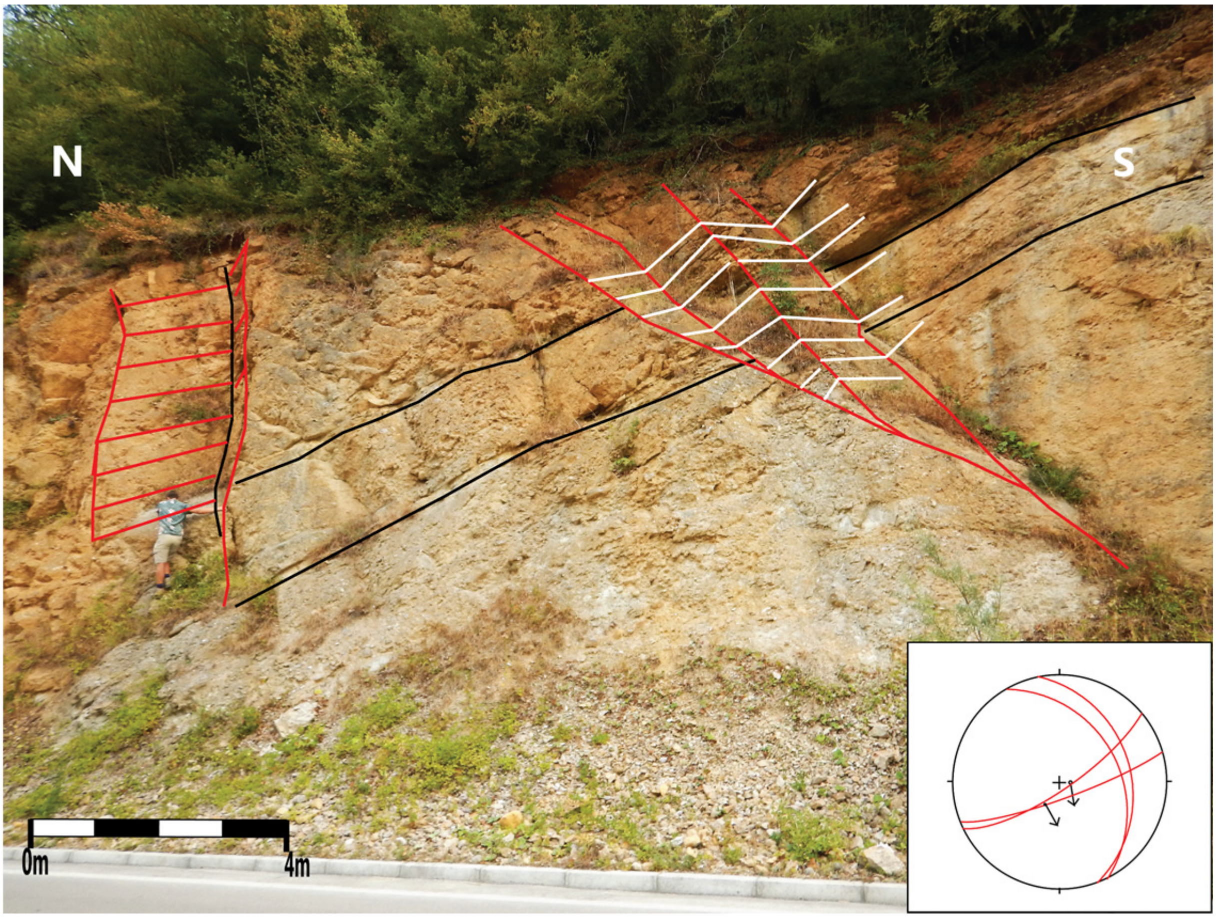

Figure 8: Field example: Extensional structures exhibiting an angular difference around 90^{o}. The fault sets are formed in high competence conglomerate deposits. Red and white solid lines are indicative to the fault plane and the black solid lines indicate the bedding planes. See figure 3 for the location.

4.2. Sedimentary environments during the Middle Miocene extension

Analysis of Middle Miocene sediments shows that the Konjic Basin is characterized by alluvial-fluvial conglomerates and sandstones that are distally replaced by deltaic and deeper lake turbiditic and lacustrine sediments (Appendix A). The sedimentary logs created in this research allow the distinction of 16 facies units (table 1). Facies units were subsequently grouped into 7 facies associations, that describe 3 depositional systems: (1) alluvial fan system, (2) deltaic system and (3) profundal lake system.

4.2.1. Facies associations

4.2.1.1. alluvial fan system

The *alluvial fan (AF) facies association* is characterized by channel to sheet-like packages of angular to subrounded, imbricated, clast dominated, pebble to cobble conglomeratic deposits alternated with medium to coarse red sandstones (Gmm, Gcm, Gp, Sm and St, table 1, fig. 9; fig. 10). The pebbles and cobbles are fragments of Variscan and post-Variscan metamorphized sediments from the Mid-Bosnian Schist Mountains and the carbonatic Mesozoic cover. The angularity of the clasts indicates that AF is deposited close to the source area. Also, angularity suggests an increase towards the NE margin of the basin. This facies association gradually passes into the delta plain (DP) facies association downslope towards the basin centre. Given the architecture of the AF facies association and the position of the Vrbas fault along the NE margin of the basin (Hrvatovic, 2006), the AF facies is interpreted to be formed by debris fall against the fault scarp (Leppard and Gawthorpe, 2006). The coarse red sandstone beds are interpreted as moments of tectonic quiescence allowing the system to rework the sediments. This phase is defined by bedload dominated small channels (DeCelles et al., 1991).

4.2.1.2. Deltaic system

The *Delta plain (DP) facies association* is characterized by large (1 to 4 m thick and >10 m wide) channelized bodies of pebble to cobble, clast-supported conglomerates. The matrix is comprised of medium to coarse red sandstone (Gmm, Gt, St, Sh and Ta – Tc, table 1; fig. 9; fig. 10). The clasts are subangular to subrounded fragments of the Mid-Bosnian Schist Mountains (MBSMs) and Mesozoic cover. Some of these subangular, elongated pebbles are imbricated, indicating paleo flow towards the south. The channelized packages record an overall fining upward trend. The DP facies association passes downslope into the proximal delta slope (DS1) facies association. These packages are deposited at the river mouth, where braided streams enter the lake (Gawthorpe and Colella, 2009). The clast-supported conglomerate is shed down during periods of active tectonics or floods (Garcia-Garcia et al., 2006). The red medium to coarse sandstone is reworked during periods of low water influx (Decelles et al., 1991).

Facies Units	Description	interpretation
Ta	coarse- to medium-grained (pebbly) sandstones with low matrix content; medium to good sorting; vertical normal grading or no grading; mud chips aligned in certain levels; erosive or planar base	Ta; High density turbidity current
Tb	Coarse- to medium grained sandstones; medium sorted; low matrix content; erosive base layer; often no grading; mud-chips	Grain to grain interaction; high density turbidity current
Tc	Medium grained sandstones; medium sorted; low matrix content; laminated; no grading	Grain to grain interaction; high density turbidity current
Td	Medium - to fine grained sandstones; good sorting; low matrix content; asymmetric ripples; cross-lamination;	Fluid turbulence; medium density turbidity current; grains reworked as bedload
Te	Fine sandstones to siltstones; medium to good sorting; graded; laminated	Fluid turbulence; low density turbidity current
Md	Siltstones to mudstones; good sorting; some degree of lamination; low grading	Fluid turbulence; mud density turbidity current
L	Mudstones; blueish colour; tabular geometry; structureless or platy; no fossils; thickness up to 25 cm.	Inorganic lake precipitation
Gcm	Mudstones; Beige colour; tabular geometry; may exhibit wavy lamination; sometimes contains ostracodes; thickness up to 20 cm	Profundal lake; particle settling from water column. (Backgroudn depostion)
Gmm	Matrix supported pebble to cobble conglomerate; subangular to subrounded; poorly sorted; amalgamation; no grading; bed thickness 1 m to 4 m.	Cohesive debris flow, where river mouth enters lake
Gp	Clast- to more matrix-supported pebble conglomerates; well rounded; imbrication; cross-bedding; Pinches out; bed thickness approximately 5 m.	Depostion from high energy bedload dominated flow in subareal to subaqueous environment (topset - foreset).
Gt	Dominantly clast dominated pebble to cobble sized conglomerate;well rounded; imbrication; eroded base;channel like geometry	Channel at distal part of the delta
Sm	Medium to coarse sandstone; often reddish; subangular grains; no structures.	Deposition at river mouth from braided or sheetflow
St	Medium to fine grained sandstones; rounded clasts; well sorted; sporadic cross-bedding; often reddish; bed thickness aroung 10 cm.	Depostion in the littoral part of the lake
Lo	Grey limestone; massive layers with wavy bottom boundaries; some beds contain oncoids	profundal lake, no continental input
Ldo	Grey limestone; massive layers with wavy bottom boundaries; with silt contamination(dirty); some beds contain oncoids	profundal lake, minimal continental input

Table 1 Facies units indicated in the Konjic Basin. Facies unit codes and their subsequent interpretation follow the general agreements of previous sedimentology studies (Bouma et al., 1962; Talling et al., 2012; Postma, 1990).

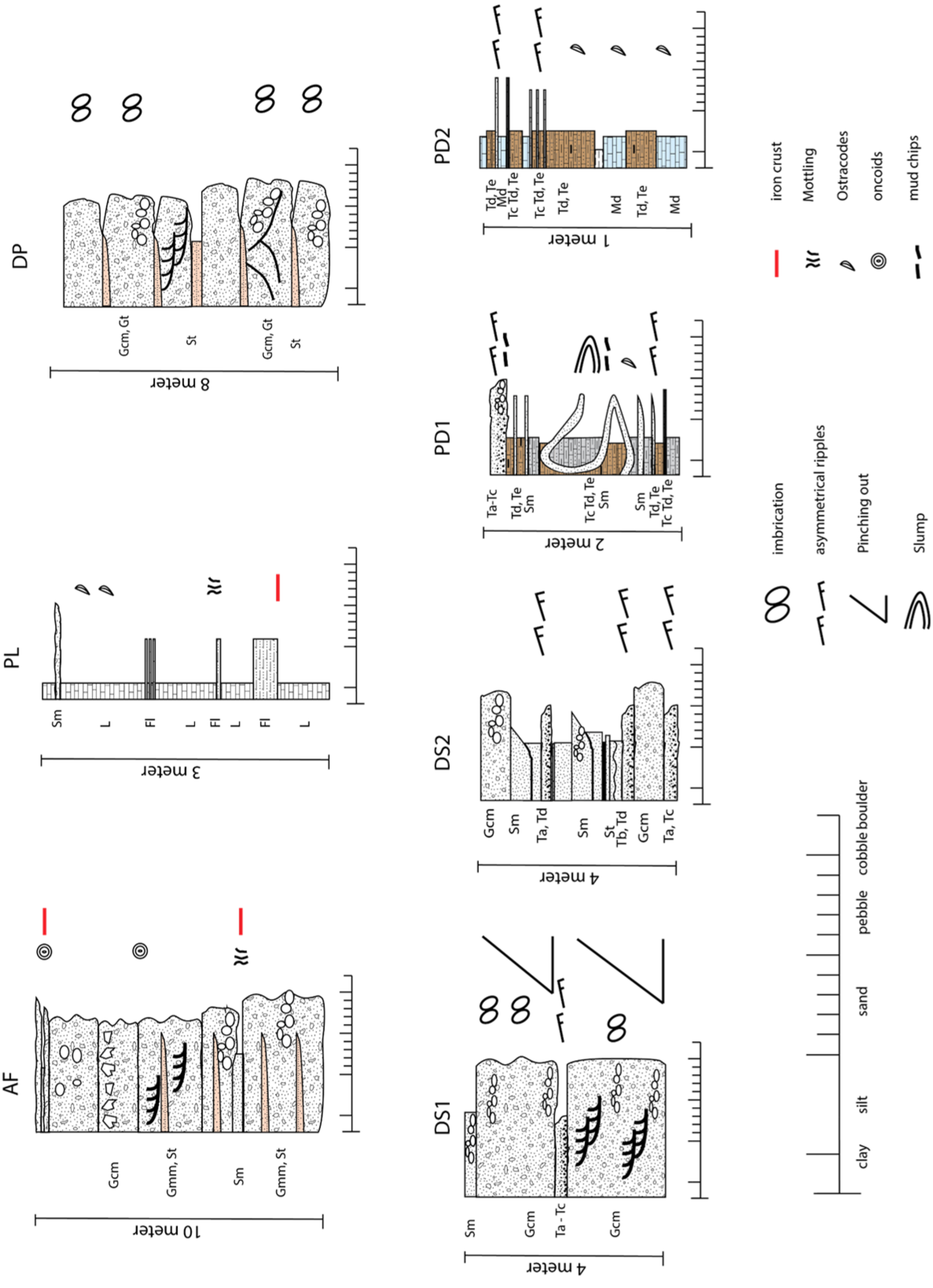

Figure 9: Illustrations of the facies association based on field observations. Grouped facies units (table 1) build-up the facies associations. AF - Alluvial fan; PL – Profundal lake; DP – Delta Plain; DS1 – Proximal delta slope; DS2 – Distal delta slope; PD1 – Proximal prodelta; PD2 – Distal prodelta.

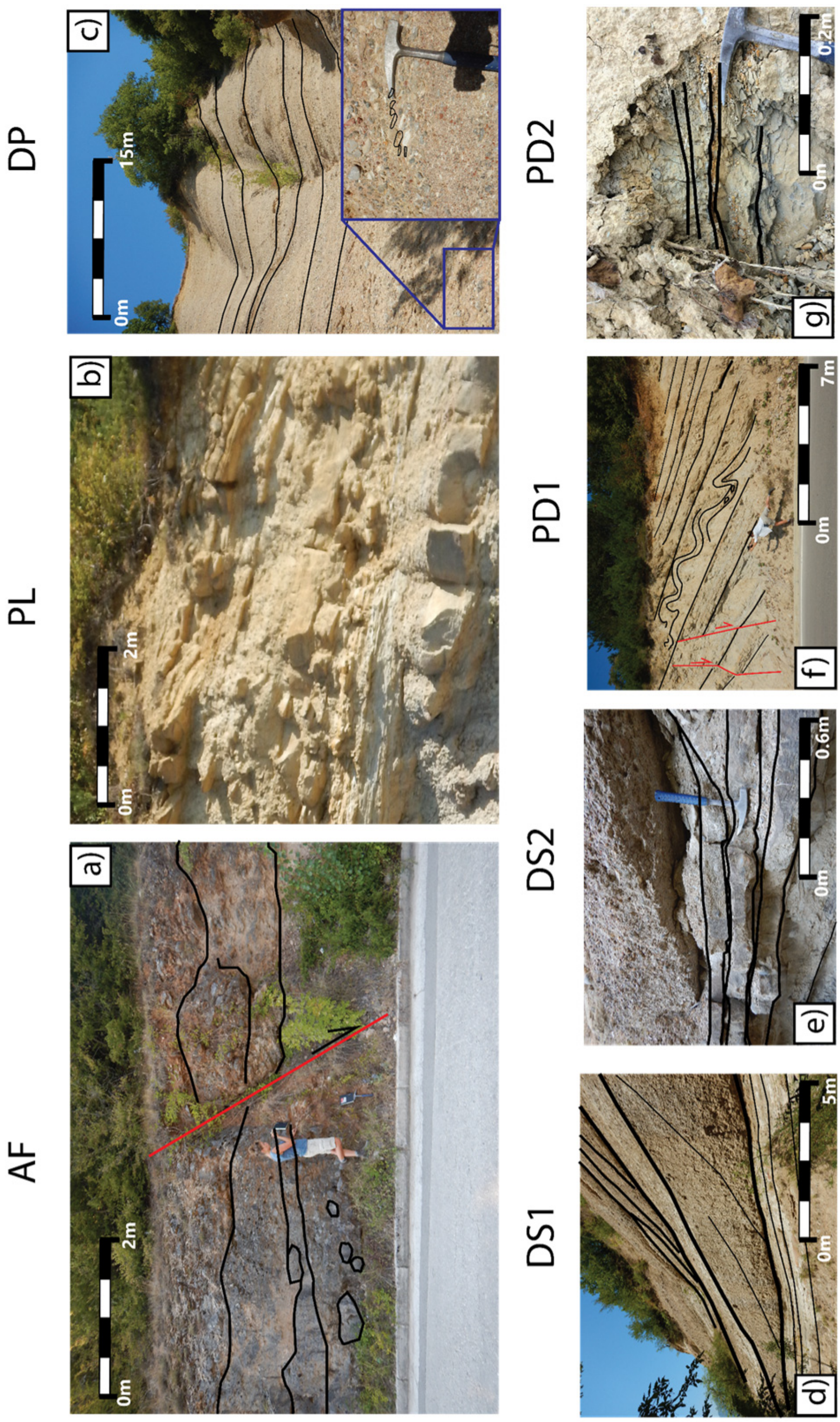

Figure 10: Field examples of facies associations recognized in the studied field area of the Konjic Basin. a) Alluvial fan facies association (AF). b) Profundal lake facies association (PL). c) Delta plain facies association (DP). d) Proximal delta slope facies association (DS1). e) Distal delta slope facies association (DS2). f) Proximal prodelta facies association (PD1). g) Distal prodelta facies association (PD2). See figure 3 for the locations.

The *Proximal delta slope (DS1) facies association* is composed of large sets of clast- to matrix-supported, subrounded, pebble-sized conglomerate alternated with medium grainsized sandstone. The geometry of the conglomerate packages is tabular, exhibiting cross beds, imbrication and tapering downslope (Gcm, Gt, Sr, Sm and Ta-Tc, table 1; fig. 9; fig. 10; fig. 11; fig. 12). Imbrication and cross bedding indicate that paleoflow is towards the south. The DS1 facies association passes into DS2 downslope and is the distal equivalent of the DP facies association. Imbricated, subrounded to subangular clasts of MBSMs and Mesozoic cover are interpreted as high energy density flow deposits (Bouma, 1964; Leppard and Gawthorpe, 2006).

Figure 11: Field example: Imbrication within proximal delta slope, indicating flow direction to the South. The figure also exhibits the subangularity to subroundness of the clasts in a sandy matrix and the alternation finer and coarser clast bands in a single flow event. See figure 3 for the location.

The *Distal delta slope (DS2) facies association* shows periodic pinching-out packages of subrounded, pebble-sized conglomerate in a medium grained, channelized and/or lobate sandstone dominated facies association (Gcm, Gt, Sm and Ta-Tc ,table 1; fig. 9; fig. 10; fig. 12). Sporadic, sandstone contains coal-rich laminae (with visible plant remnants). The sandstone occasionally exhibits ripple structures and some layers contain outsized pebbles of MBSMs origin. DS2 gradually passes into PD1 downslope. The outsized pebbles and small conglomeratic beds on top of the relative finer channelized and lobate sandstone beds is interpreted to be the result of surge-like turbidity currents. Flooding events or enhanced sediment input, lead to bypassing of the proximal part and high energy deposits (Leppard and Gawthorn, 2006). The flow of a surge-type turbidity current, under certain circumstances, can divide into a denser, non-turbulent layer and an upper, less dense turbulent layer. Outsized clasts trapped between these two layers, can glide/float along this interface and get transported further downslope than the pebble-size at first sight insinuates This mechanism enables medium energy turbidites to carry pebbles/cobbles, associated with high energy turbidites, downslope (fig. 13; Postma et al., 1988).

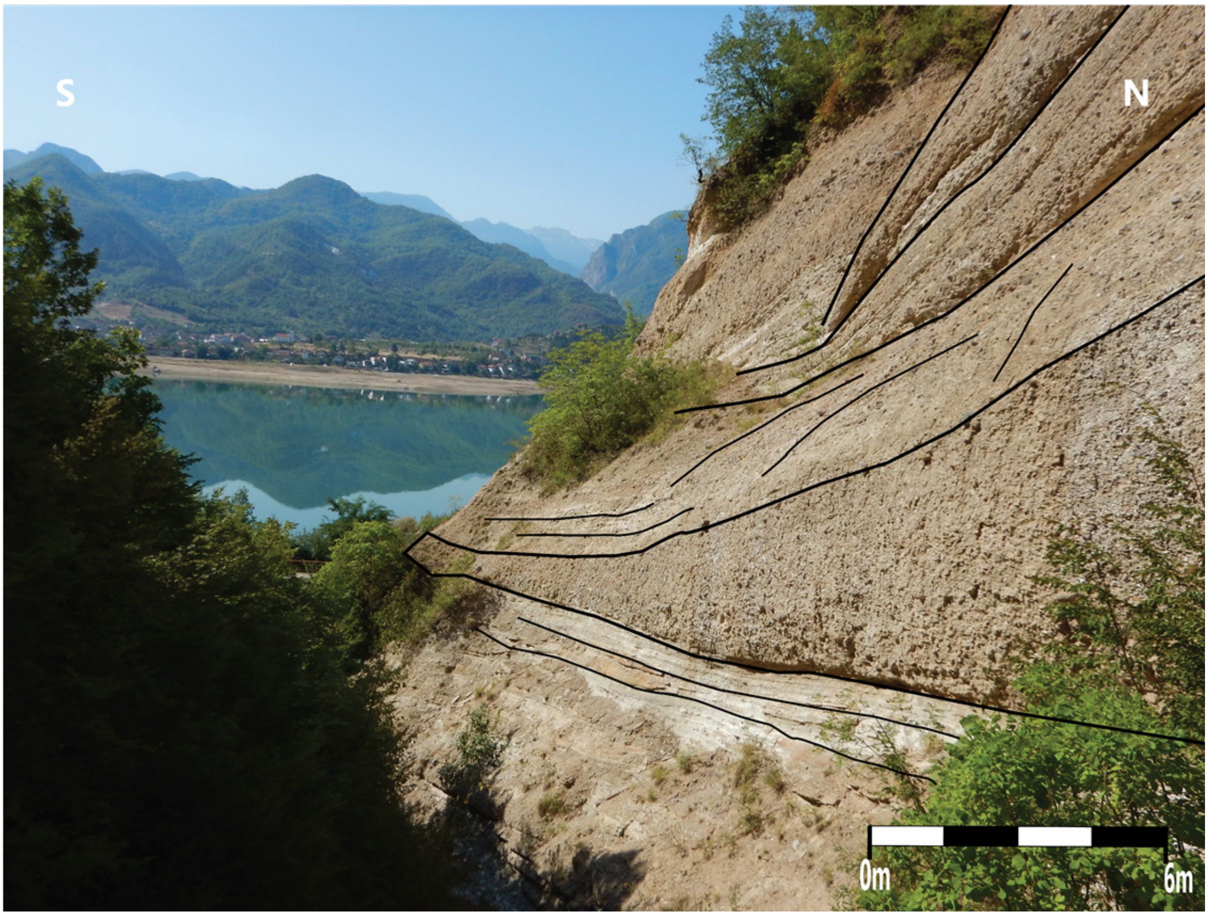

Figure 12: Field example: Proximal delta slope deposits tapering towards the south in the direction of flow. Note the decrease in grainsize and therefore in energy of the flow towards the south and the transition towards the distal delta slope facies association within 25 m. Also note the vertical evolution of this outcrop. Thick packages of DS1 and DS2 alternate, which is reflected in the sedimentary log as fining- and coarsening upward cycles. See figure 3 for the location.

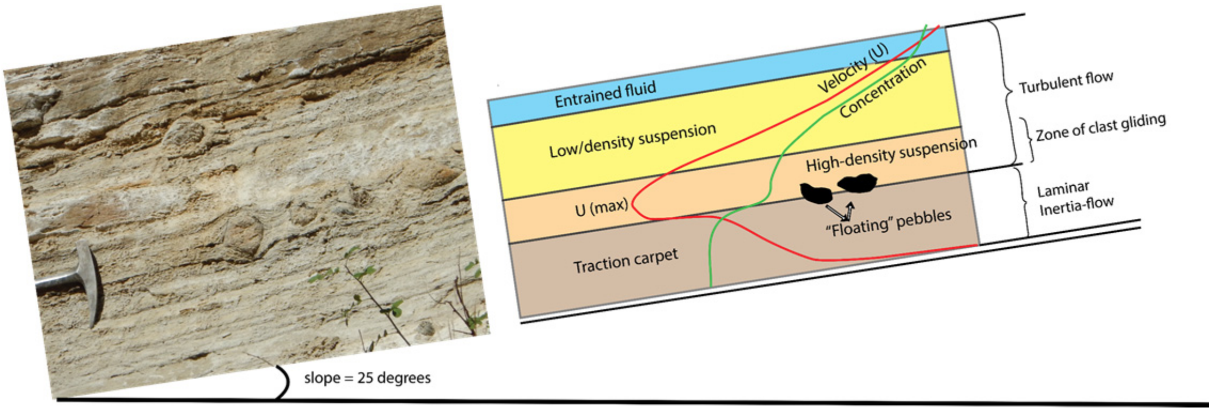

Figure 13: Field example: Photo taken underneath the delta slope deposits of figure 12, showing "floating pebbles" in distal delta slope facies association. Illustration modified after Postma et al. (1988), explaining the occurrence of cobbles in coarse sands. Flow of a high-density turbidity current naturally divides into a turbulent flow at the top and a laminar flow at the bottom. Clasts trapped in the zone between, "zone of clast gliding", are transported further downslope than equally sized clasts in the bottom or top layer. See figure 3 for the location.

The *Proximal prodela (PD1) facies association* contains sheet-like alternations of marly limestones and silty marlstone. It shows sporadic occurrences of channel and lobate structures and (medium to) fine sandstone ripple geometries (Ta-Te and Sm, table 1; fig. 9; fig. 10). Slumps, associated with the proximal prodeltadeposits, interrupt the repetitive sequence (fig. 7c). Slumps are made-up of marly limestones as well as medium grained sandstone and contain rip-ups clasts (<5cm) of intra-basinal semi-consolidated silt- and claystones. PD1 gradually passes from DS2 into PD2 and is sometimes intercalated with profundal lake facies association (PL). Toe slope deposits as well as small channels and lobate geometries reveal that deposition is in the proximal part of the prodelta (Talling, et al, 2012).

The *Distal prodelta (PD2) facies association* is comprised of sheet-like and occasionally lobate alternating packages of (fine sandstones) silt- and mudstones (Tc, Td, Te, Md, L, Lo and Ldo ,table 1; fig. 9; fig. 10). Some claystone layers exhibit paper-like parallel lamination with sporadically organic matter , whilst other darker claystones contain ostracods. The silt- and mudstones indicate that the energy of the environment is very low, although the fine sandstone layers reveal some periods of disturbance of very low density turbidity currents (Bouma, 1964; Talling et al., 2012). The paper-like claystones reveal deposition from particle settling from the water column (Melchor, 2007).

4.2.1.3. Profundal lake system

The *Profundal Lake (PL) facies association* shows alternations of marly limestones that sometimes contain dispersed organic matter and blueish silty marlstone with more organic remnants (Fl, Md, L and Te, table 1; fig. 9; fig. 10). The silty marlstones occasionally contain small red layers and mudstones sporadically contain ostracods. The main inferred depositional process is particle settling from the water column in a low energetic environment (Postma, 1990; Talling et al., 2012). The PL facies is repetitively disturbed by PD2 and PD1 facies associations as a consequence of enlarged sedimentary input and can be interpreted as progradation of small delta into shallow lake or occasional storm events (Melchor, 2007).

4.2.2. P-R cycles

The detailed description of the sedimentary record in terms of facies units and facies associations allowed the recognition of rhythmic coarsening and fining upward trends. One coarsening upward sequence followed by fining upward is called a progradation-retrogradation cycle (P-R cycle). 6 P-R cycles were recognized and described in sedimentary logs (Appendix A). One P-R cycle is found in the alluvial-fluvial environment (AF to DS2) (fig. 19a). Another five P-R cycles are found in more low energy environments (DS2 to PD2). The architectural geometry of a second-order cycle in the proximal part of the basin is not comparable with the same order cycle in the distal part of the sedimentary system. Figures 19a; 19b; 19c clearly illustrate the pinching out of large (2+ meter thick) conglomerate beds over a distance of 25 meters into decimetre scale sandstone beds encapsulated by distal deltaic strata. This visualizes that sedimentation rates in the distal part (PD2, PD1, PL) of the sedimentary system are clearly of a lower rate than the sedimentation rates in the deltaic and alluvial part of the system. Latterly the transition of one P-R cycles from the alluvial to the distal prodelta facies association is over approximately 500 meter. Based on lithostratigraphic age and fault kinematics, the P-R cycle observed in the proximal part (fig. 19a) is laterally not linked to any of the five distal P-R cycles. The distal P-R cycles are captured in large scale outcrops (13m to 25m thick) and are presented in figures 14 and 15. Magnetostratigraphic correlation in the neighbouring Sarajevo-Zenica basin indicated sedimentation rates of 40 cm/kyr in the distal part of the sedimentary system (Sant et al., 2018). This rate is adopted by our study to put a time restraint on the five P-R cycles recorded in the distal environment and revealed a total depositional time of approximately 125 ky. Figure 14 exhibits two and a half P-R cycle in the deltaslope facies associations (DS1 & DS2). Also, a general fining upward trend is recognized and interpreted as retrogradation of the depositional system (fig. 14). The other eminent characteristics of this log are the conglomerate package characterized by an erosional base and a slump, both preluding retrogradation. The erosional surface is rough and the conglomerate exhibits rip-ups in the base, distinguishing these beds from channelized DP and DS facies association beds. The slumps described in the prodelta facies association and the coarse conglomerate packages are associated with slope instability and mark depositional events during the Middle Miocene in the Konjic Basin. Figure 15, similar in the sense that progradation is followed by retrogradation of depositional system, differs from figure 14 when considering the overall trend. This log exhibits an overall coarsening upwards trend. The log is described as distal and proximal prodelta (DS1, DS2 & PD1) passing into delta slope facies associations and contains one complete and one unfinished P-R cycle. The retrograding part of the cycle is yet again preceded by a thick conglomerate package with an erosional base, containing large clasts of Middle Miocene material that was scrapped off the bottom and transported downslope with the rest of the coarse package during deposition. In the more distal facies associations these trends are interrupted by thin (<20cm) intervals of coarser material.

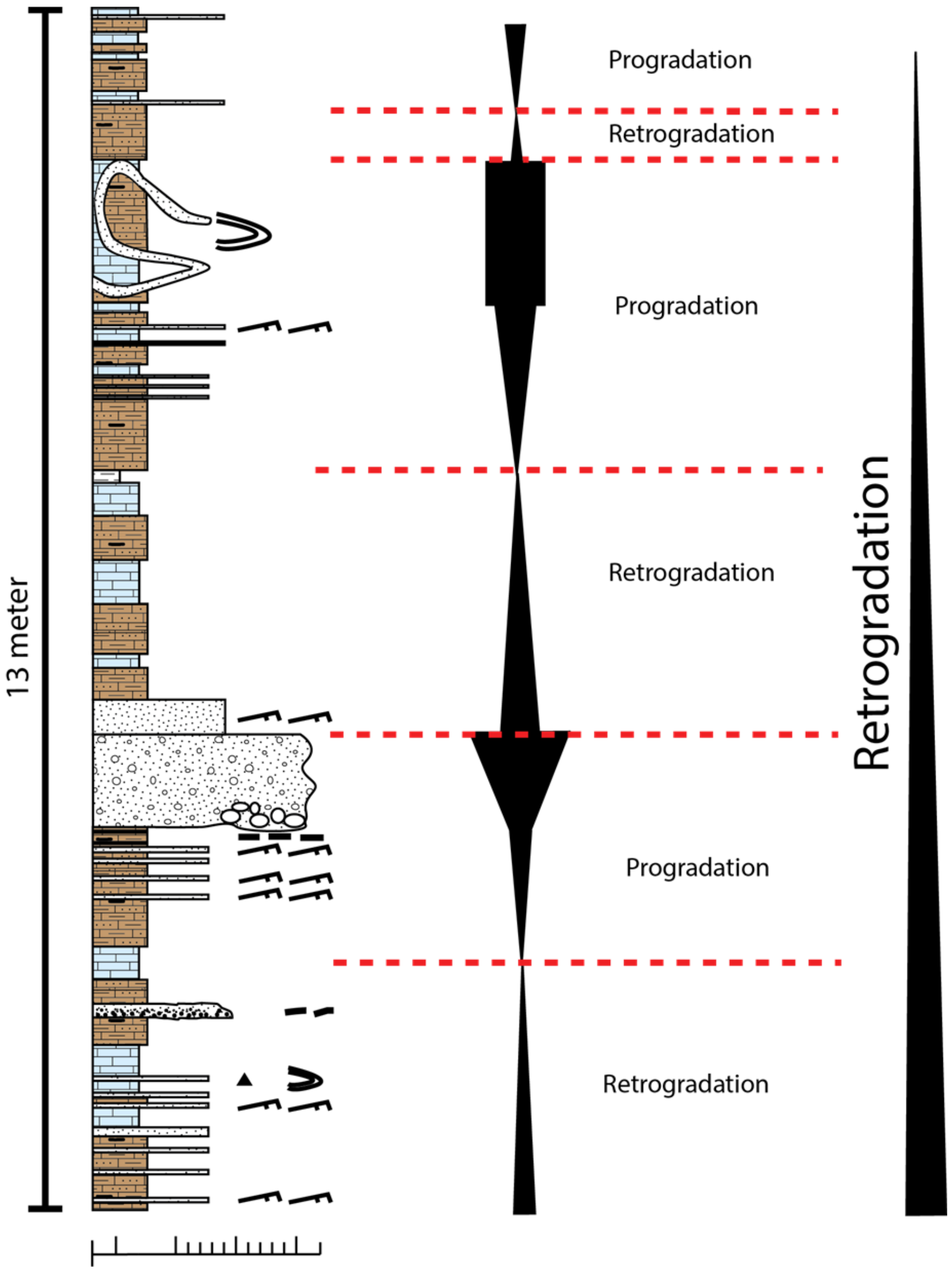

Figure 14: Part of log A4 showing prodelta to distal delta slope deposits disturbed by coarse packages and slumps. Dotted red lines indicate the transition of the system from progradation to retrogradation and vice versa. When neglecting the outsized beds, the overall trend is fining upward (Retrogradation). Note that the outsized bed and the slump both prelude a period of retrogradation. See figure 3 for location of log A4. The complete log A4 can be found in Appendix A4.

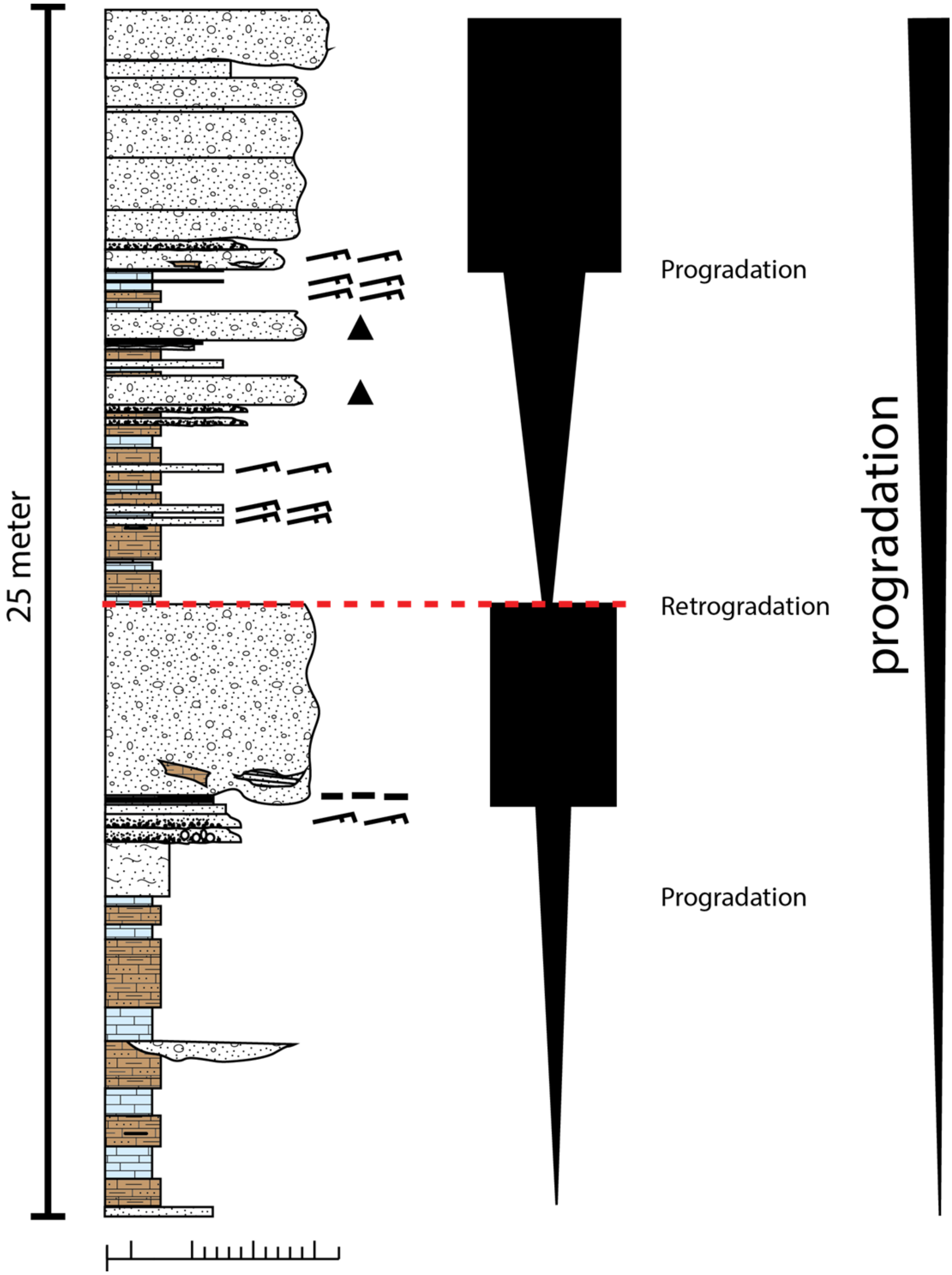

Figure 15: Part of log A4 showing profundal to proximal delta slope deposits disturbed by thick coarse packages. Dotted red lines indicate the transition of the system from progradation to retrogradation. Retrogradation is limited to a brief moment immediately after the deposition of a thick coarse packages. The overall trend is coarsening upward (Progradation). Note that the outsized bed preludes a moment of retrogradation. See figure 3 for location of log A4. The complete log A4 can be found in Appendix A4.

5. The link between Middle Miocene extension and evolution of facies associations

Field observations in the Konjic Basin show a close link between deposited facies associations and normal fault activity. The sedimentological and kinematic data revealed that accommodation space, created by normal faulting, is filled-up while movement along the fault is still taking place (fig. 6a; fig. 6b; fig. 7a; fig. 7c). The P-R cycles linked to the activity of a set of related normal faults are referred to as second-order P-R cycles. Together these second-order P-R cycles make up a first-order cycle that is controlled by the imbalance between accommodation space and sedimentation on basin scale.

5.1. Second order P-R cycles

By combining the P-R cycles from figures 14 and 15 with the syn-kinematic observed normal faults in the field, this study was able to link almost all the P-R cycles directly to normal fault activity. The combined data shows fault activity preceding deposition of relative coarse packages and slumps (figures 16 and 17). Since normal faults responsible for observed sedimentary structures are not always present in the same outcrop, the unique sedimentary responses of more immature packages and slumps were used as indicators for tectonic activity. These sedimentary structures show a similar architecture compared to sedimentary structures where the syn-kinematic normal faults were present. These outstanding sedimentary structures were created by basin-ward shed energetic flows, inferring slope instability due to normal fault activity. This study distinguished three units A, B and C (fig. 16) indicative for fault related slope instability and revealed six second order P-R cycles (fig. 17).

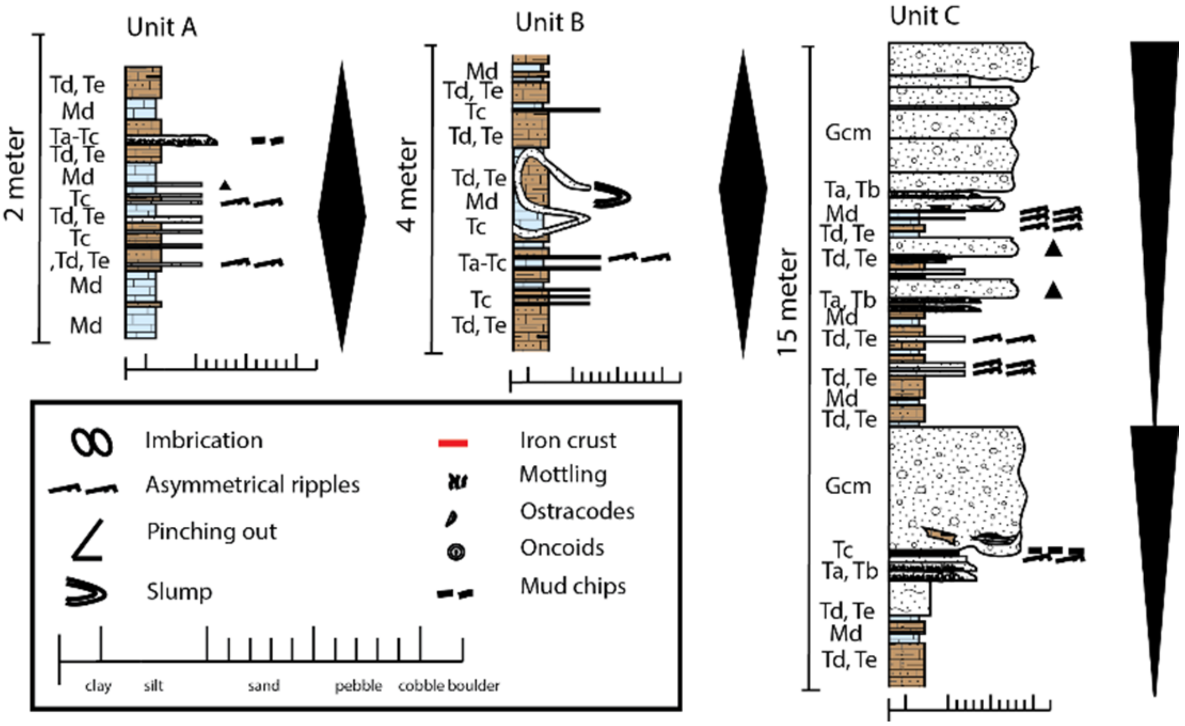

Figure 16: Three typical units distinguished in the Konjic Basin indicative for slope instability. Unit A – observed in the distal prodelta. Silt and mudstones are disturbed by period of increasing amount of sandstone deposits generating asecond-order P-R cycle. Unit B – Observed in the proximal delta slope. Silty and sandy deposits are interrupted by a slump inferring slope instability. Unit C – Observed in the proximal prodelta to delta slope. Obvious coarsening upward trend that is interrupted by a sudden transition to silty and sandy deposits. The large rip-ups and shear structures at the base of the thick coarse package of conglomerate in a sandy matrix underline slope instability.

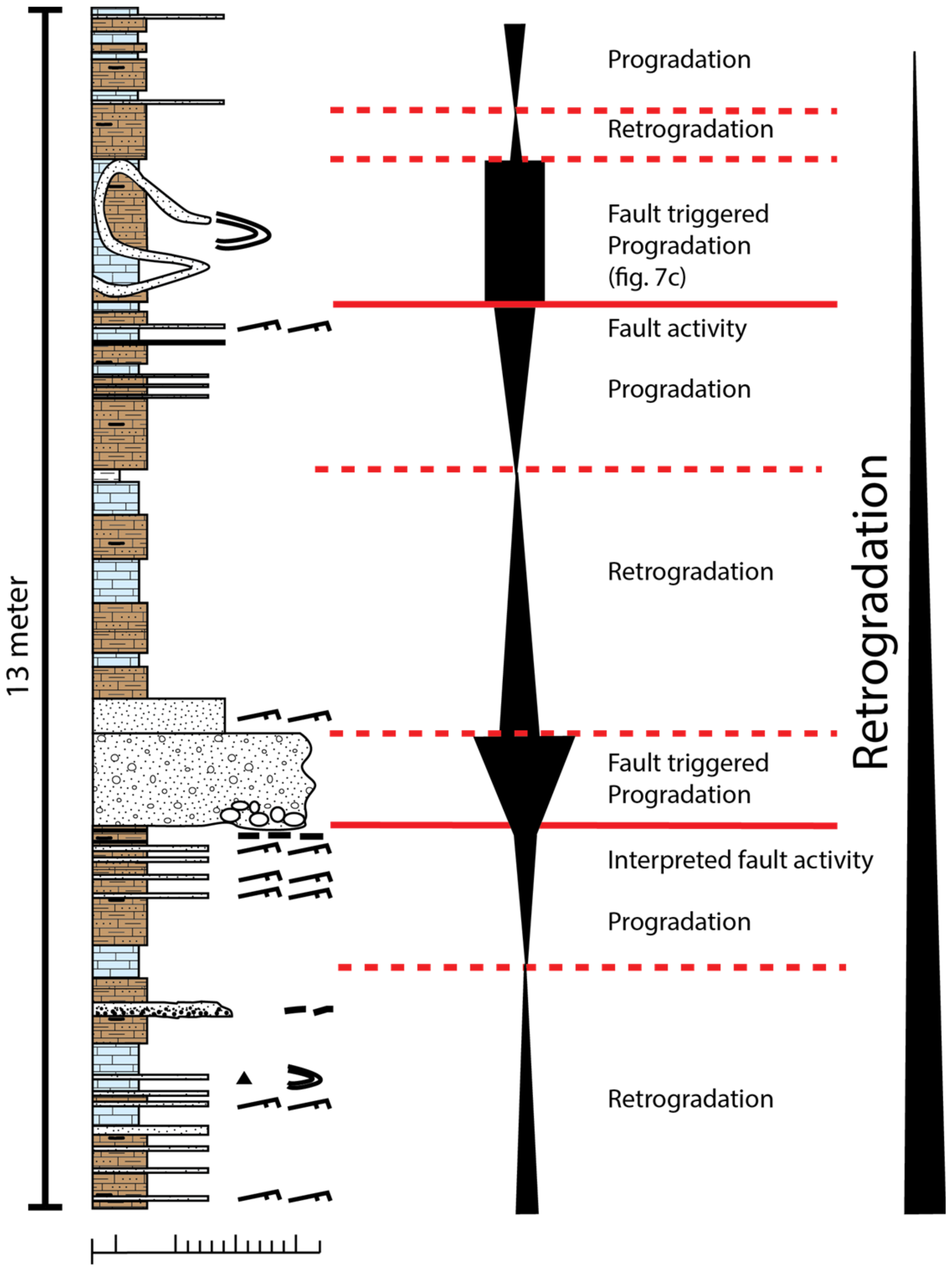

Figure 17: Part of log A4 showing prodelta to distal delta slope deposits disturbed by coarse packages and slumps. The overall trend of the log is retrograding. In more detail the sedimentary succession exhibits from bottom to top: retrograding and prograding cycles. Packages of coarse material are shed down and alternate with prodelta and profundal lake deposits. The combination of our sedimentological and kinematic data revealed that there is a causal link between normal fault activity and the sedimentary profile found. Observed faults are linked to observed sedimentary geometries. Where faults were not observed, these are interpreted based on sedimentary geometry similarities to other sedimentary geometries that did show a clear relation between normal faulting and sedimentary response. See figure 3 for location of log A4. The complete log A4 can be found in Appendix A4.

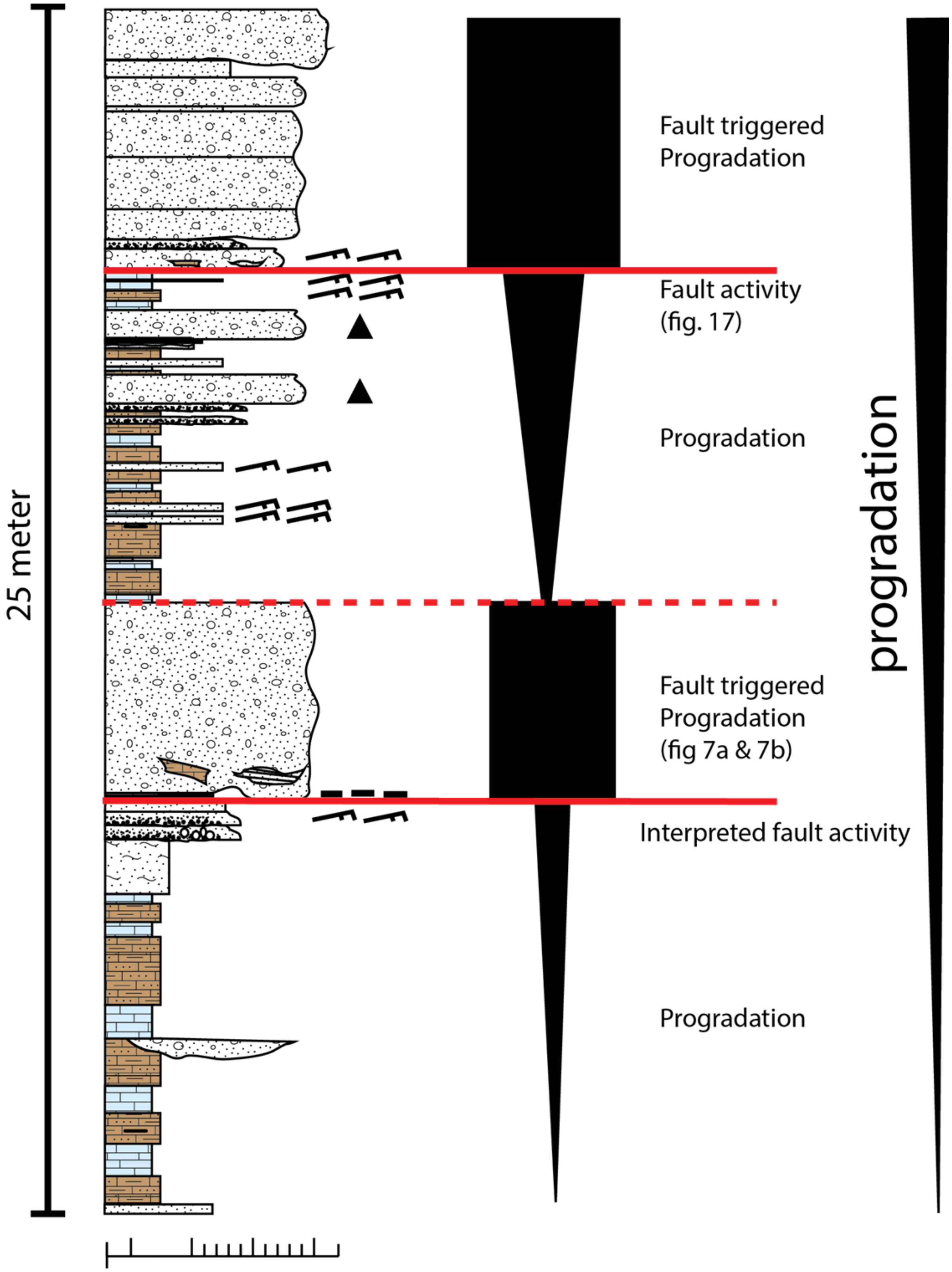

Figure 18: Part of log A4 showing profundal to proximal delta slope deposits disturbed by thick coarse packages. The overall trend of the log is prograding. In more detail the sedimentary succession exhibits from bottom to top: progradation followed by moments of retrogradation. Packages of coarse material are shed down and alternate with prodelta and deltaslope deposits. The combination of our sedimentological and kinematic data revealed that there is a causal link between normal fault activity and the sedimentary profile found. Observed faults are linked to observed sedimentary geometries and interpreted as the driving mechanism for these progradation – retrogradation cycles. See figure 3 for location of log A4. The complete log A4 can be found in Appendix A4.

5.2. First-order P-R cycles

The sedimentary record in Figure 17 is interpreted to show retrogradation in a first-order P-R cycle, whilst the record in figure 18 shows the progradation part of a first-order P-R cycle. The first-order retrograding trend in figure 17 results from the accommodation space being larger than the sediment supply. This phase is interpreted as a normal faulting climax phase with resultingly deepening of the basin (Prosser, 1993). The basin deepening is succeeded by first-order progradation (fig. 18). This phase is interpreted as the waning stage of faulting where sediment supply becomes larger than accommodation space. This is also seen in other basins such as the Sarajevo-Zenica Basin (Andrić et al., 2018) and described by Prosser, (1993) (and references therein) as typical basin development.

The Middle Miocene Konjic Basin follows the typical development of an intra-montane basin (see also Garcia-Garcia et al., 2006). A period of high subsidence, controlled by normal (growth) faults producing retrograding units, is followed by a period of low subsidence. The decrease in accommodation space produces prograding deltas (Garcia-Garcia et al., 2006). The period of basin deepening is characterized by an unique evolution of sedimentary environments. The activity of normal faulting is exhibited in both the deltaic environment as in the lateral deeper, prodelta facies associations. The waning stage of normal fault activity is recorded by prodelta going into delta slope facies associations and marks the shallowing of the basin. In order to construct an evolutionary model for the Konjic Basin, both the first-order retrogradation and progradation are investigated in detail.

5.2.1. First-order retrogradation

The high activity of normal faulting during the Middle Miocene increases the accommodation space rapidly, initiating a first-order retrograding pattern. The pattern is recognized in the sedimentary record as overall fining upward and is alternated by more immature and coarse packages associated with moments of fault activity (fig. 17). Facies associations migrate in a basin-outward direction. Synchronous relations between sedimentary deposits and normal faults linked the deepening of the basin to NNE-SSW and NE-SW first and second phase of extension (fig. 4.1; fig. 4.2).

A conceptual model illustrating the lateral and vertical facies association evolution during the deepening of the basin is presented in figure 20. In this model, retrogradation in the proximal part of the basin is recognized by immature alluvial fan deposits laterally and vertically passing into fluvial and subsequently deltaic deposits. Normal faulting caused either the slope increase on the deltaslope facies associations by deepening of the basin or footwall uplift, or a combination of both. The coarse-grained ~30° slope, isolated fan- to wedge-shaped deltaic geometry (fig. 19), suggest a Gilbert-type delta (Breda et al., 2007) Gilbert-type deltas consist of thin, (sub-)horizontal topsets, relative thick steeply dipping and prograding foresets, and (sub-)horizontal bottomsets (fig. 19). This delta-type often forms in lakes where river water enters the basin (Gawthorpe and Collella, 2009). To create progradation in an overall deepening basin, observed in this proximal environment, large footwall erosion rates are required (Leppard and Gawthorpe, 2006). The topset, consisting of subangular subrounded conglomerate, starts flowing or avalanching with the input of new clasts or when the slope is over-steepened. Sediment is shed basin-wards by a combination of sediment gravity flow, slumping and high-density turbidity currents (McConnico & Bassett, 2007). Figure 11 and figure 13, showing tapering of imbricated cobble to pebble-sized beds in a sandy matrix, suggest that debris flow is the main mechanism for deposition on the foresets in the deltaic system. The debris flow continues further downslope and most of its energy and cohesion is dissipated the moment it reaches the bottom sets (figs. 12, 13, 19). At this point the debris flow has evolved in a high energy turbidity current. At least 5 single debris flows can be distinguished in figure 19a. Each flow is followed by a period of quiescence, leading to a successively coarsening and fining upward pattern defined as higher-order P-R cycles. Figures 19b and 19c illustrate that the progradation and retrogradation difficult to recognize in a log showing small scale faults, but 5 smaller flow/avalanching events have been observed at larger scale (in combination with figure 19a). The 5 individual packages are interpreted as the response to one genetically related set of faults or perturbation on its slip rates. The entire outcrop is one second-order P-R cycle response.

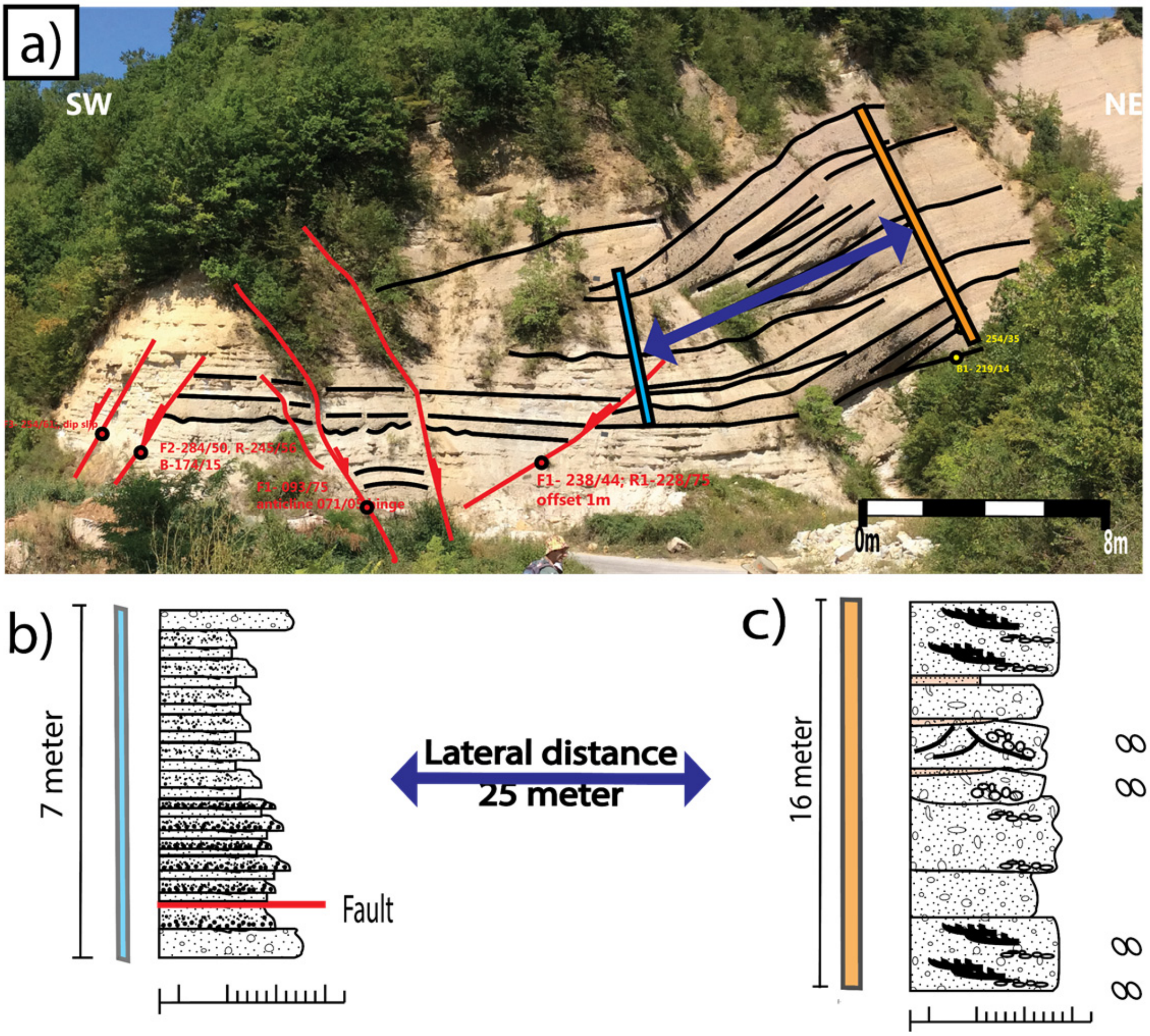

Figure 19: a) Outcrop exhibiting lateral transition from delta slope into prodelta facies associations during normal faulting climax. b & c) Logs, exhibiting the architectural difference between the proximal and distal delta slope response to slope instability. This is clearly illustrated by the pinching out of the coarse grained delta slope facies into finer distal delta slope and prodelta facies. See figure 3 for the location of 19a-c.

In the more distal part of the sedimentary system, retrogradation is associated with an overall fining upward trend from the deltaic towards the prodelta and profundal lake environments. The progradation patterns, associated with footwall uplift and slope steepening as a response to normal faulting indicated in the proximal environment, consequently influence the more distal depositional environments. This is best reflected in the sedimentary record of the profundal lake that shows an overall fining upward trend alternating with thick packages of coarse material or slumps inferring fault activity (fig. 7; fig. 17; fig. 18). For example, slumps (fig. 16 - unit B) often found on top of small offset normal faults (fig. 7c) are indicative of normal fault activity.

However, footwall uplift is not the only mechanism that can shed sediments basin-wards. Other mechanisms include (1) flood-surge events (Støren et al., 2010; Leppard and Gawthrope, 2006), (2) autocyclic avulsion of lobes (Bryant et al, 1995) and (3) wave (ravinement) erosion of the shoreline as a consequence of relative base-level rise. The latter mechanism deposits are so-called “healing phase” sediments (Catuneanu, 2002). All three transport mechanisms give rise to the shedding of coarser material into the basin leading to coarsening upward trends.

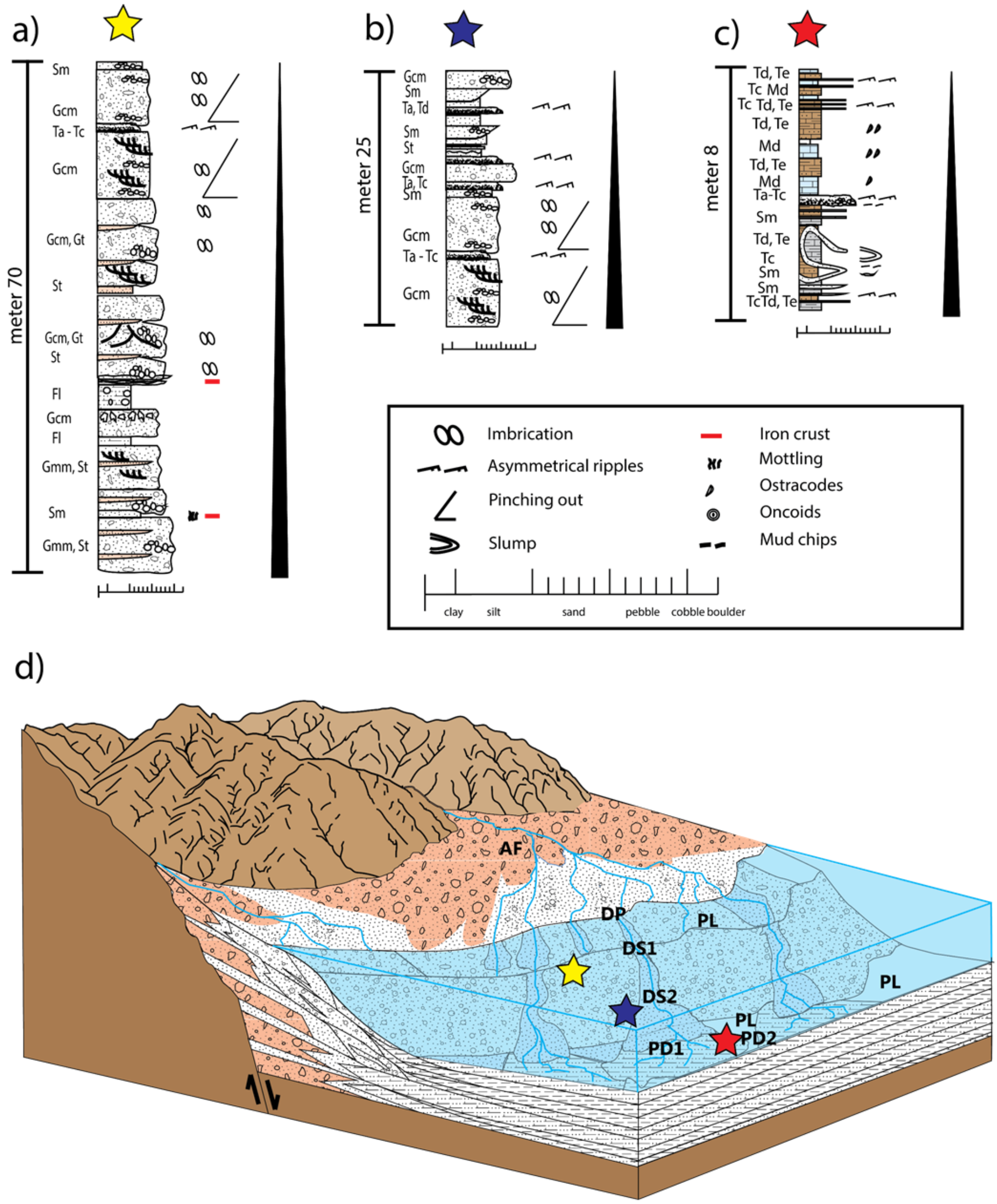

Figure 20: a) Typical log that is associated with the deepening of the basin exhibiting the transition from alluvial deposits into proximal deltaic associated sediments. b) Typical log illustrating a fining upward trend on the delta slope formed during continuous deepening of the basin. c) Typical prodelta log illustrating repeatedly profundal lake and turbiditic sediments disturbed by a slump. d) Conceptual depositional model illustrating typical retrogradation depositional trend in an asymmetric basin during normal faulting climax with major footwall uplift based on field observations in the Konjic Basin.

5.2.2. First order progradation

The final stage of Middle Miocene basin evolution is controlled by the termination of fault activity, referred to as the waning stage of normal fault activity. The NE-SW extensional direction is linked to the second phase of normal fault extension. Low rates of accommodation space creation and ongoing sediment supply initiate the prograding part of the first-order R-P cycle. It is recognized by its typical overall coarsening upward trend and migration of the facies associations basin-wards.

Lateral and vertical changes in facies associations are captured in a conceptual model for the waning stage of faulting (fig. 22). In this model, the first-order progradation in the proximal part is recognized by deltaic deposits passing vertically and basin outward into alluvial fan deposits (figs. 18 and 21). The clasts of the alluvial-fluvial facies association are more mature than the clasts deposited during first-order retrogradation. This indicates an increase in transport. The grainsize reduction can also be caused by a decrease in elevation of the source area (Catuneanu, 2002).

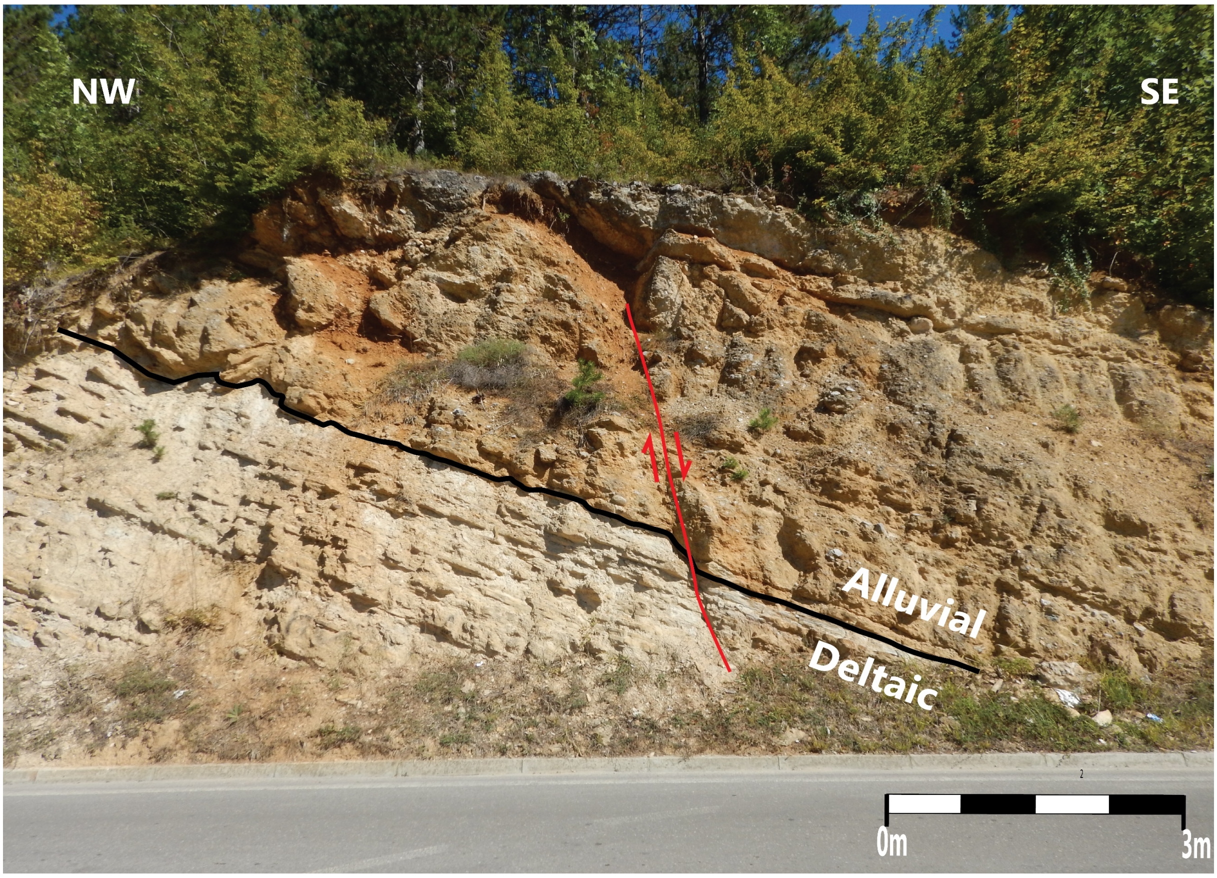

Figure 21: Field example of a top to the SE normal fault cross-cutting the transition from deltaic to alluvial. The offset of the fault is minor (15 cm).The transition is associated with the waning phase of normal fault activity that leads to the gradual filling-up of the basin. See figure 3 for the location

The more distal facies association (PD2, PD1, DS2) reflects the development to a waning faulting stage by an overall coarsening upward trend in the sedimentary record, vertically passing into delta slope deposits (DS2 and DS1) (fig. 16a). Detailed examination revealed that the sedimentary record is controlled by a similar process causing the progradation retrogradation pattern observed during the deepening of the basin. Unit C from figure 16 clearly illustrates that during system instability, interpreted as normal fault activity, coarse material is shed basin-wards. The balance between accommodation space and sedimentation is in this case directly restored, filling-up the created accommodation space almost instantaneous leading to an overall prograding part of a first-order cycle.

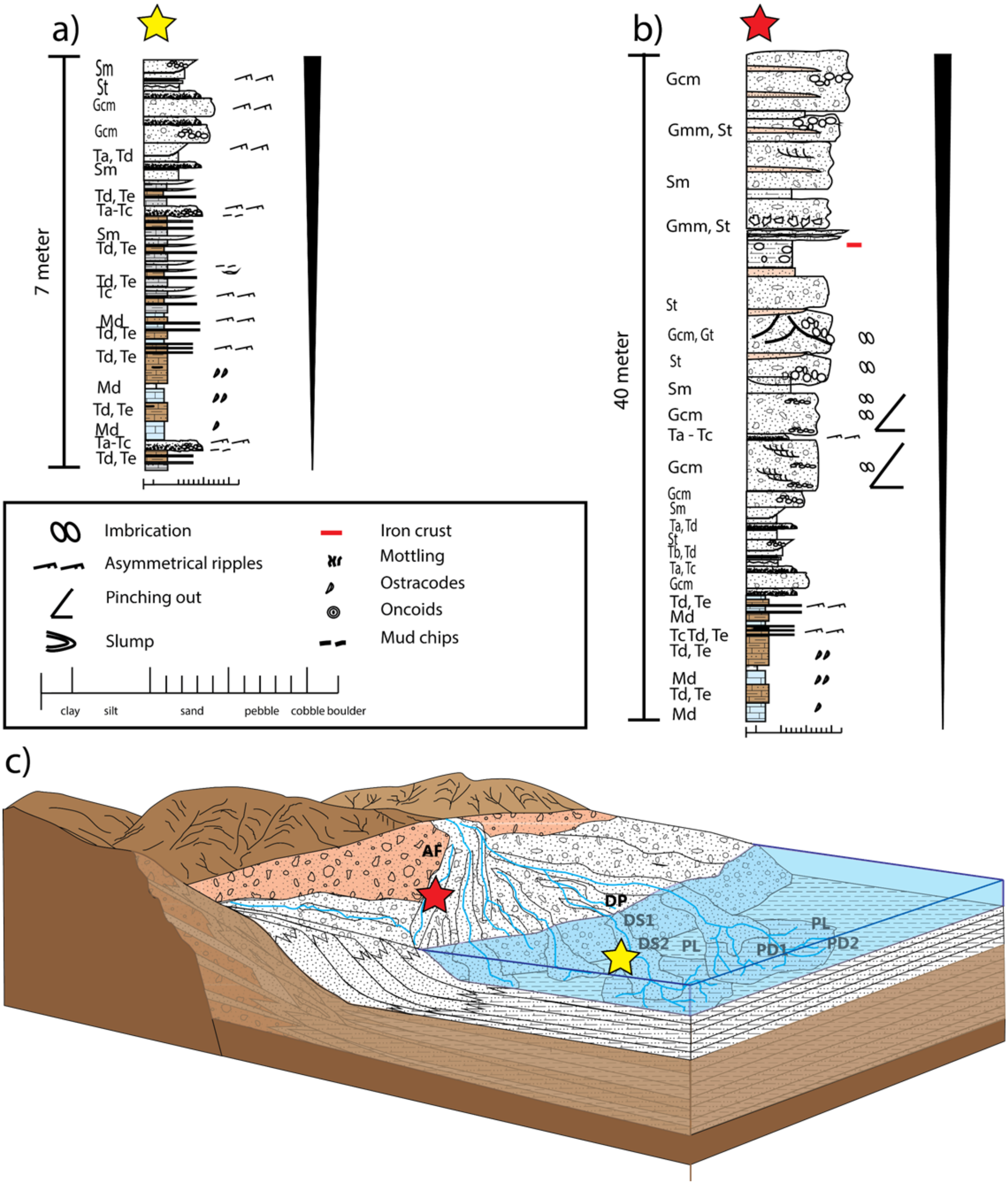

Figure 22: a) Typical log that is associated with the filling-up of the basin exhibiting the transition from prodelta (turbiditic) deposits into distal delta slope associated sediments. b) Typical log illustrating a coarsening upward trend from prodelta facies association gradually into fluvial-alluvial sediments. c) Depositional-model illustrating typical prograding depositional trend in an asymmetric basin following termination of faulting activity with limited footwall exhumation and erosion based on our observations in the Konjic Basin.

5.2.3. Cross-sectional model

A cross-sectional model is proposed that accounts for the first and second-order P-R cycles in the Konjic Basin including the higher order P-R cycles observed in the proximal environment (fig. 23). The model is kept as simple as possible, without deformation migration and climatic effects. It illustrates the results of the interplay between normal faulting and footwall uplift creating the observed kinematic extensional structures and Middle Miocene sedimentary environments and geometries.

The 6 moments of activity that were detected by this study are a minimum amount in the Konjic Basin, since this study was not designed to construct a continuous log throughout the entire basin. A total of four second-order P-R cycles is recognized in the strata associated with high amount of fault activity and deepening of the basin (Appendix A3). Two second-order P-R cycles are found in the waning stage of faulting associated with the filling-up of the basin (fig. 18).

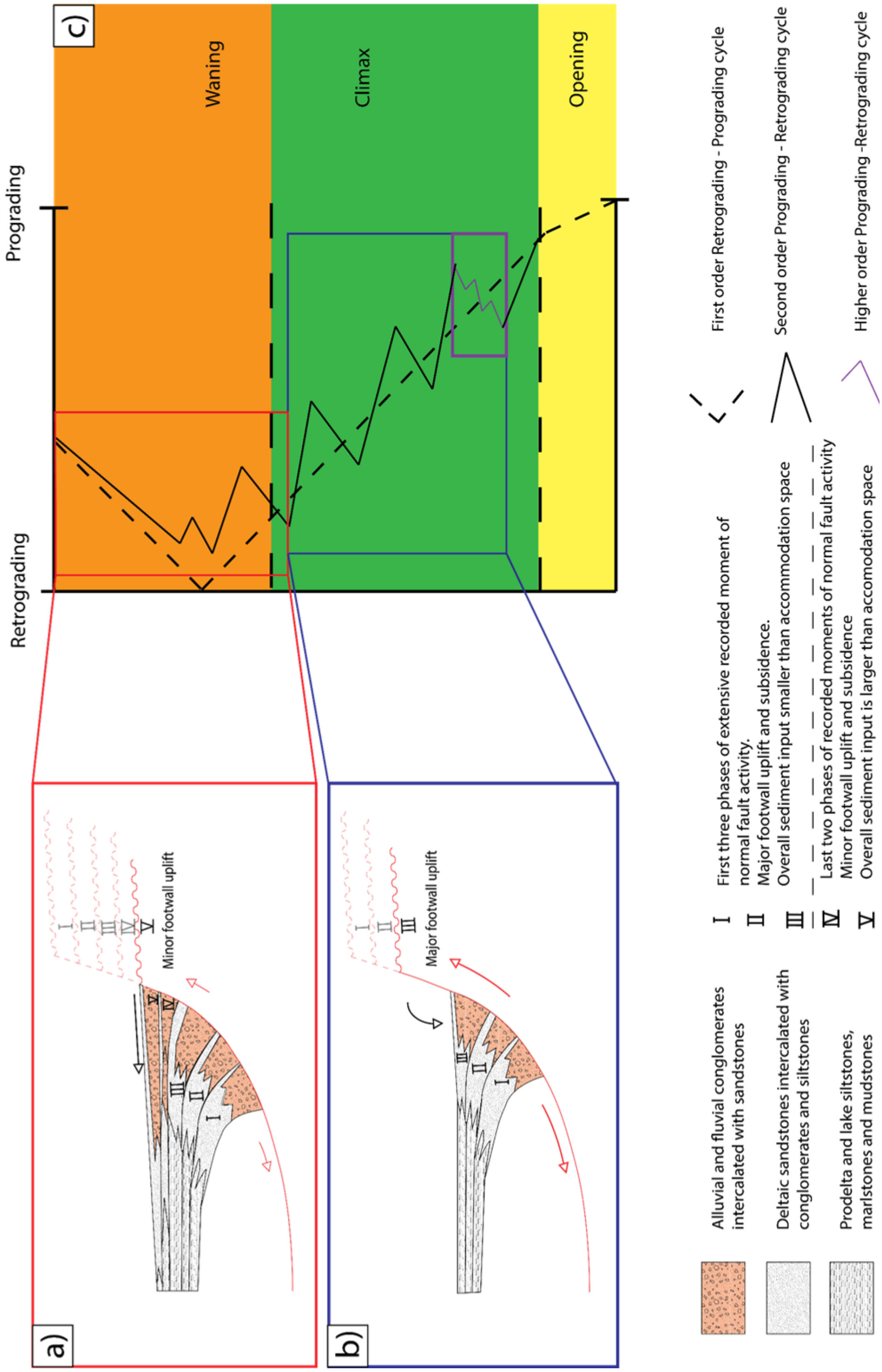

Figure 23: 2D conceptual depositional model combining the deepening and filling-up of the basin during Middle Miocene extensional phase in the Konjic basin. The model is divided into 5 moments of major normal fault activity based on the second order P-C cycles that this study indicated. a) Three moments of normal faulting/basin subsidence and coeval major footwall uplift. Note the Basin outward migration of facies. The second order P-R cycle defined as i, ii, and iii show progradation followed by retrogradation. This study has shown that the moment of normal fault activity is indicated by coarse packages shed basin-wards. Overall accommodation space is larger than the sediment input from the footwall, depicting the retrograding part of a first-order P-R cycle. b) Two moments of minor normal faulting and coeval minor footwall uplift. The second order P-R cycles are defined as iv and v and show coarsening upward and basin-wards migration of facies associations. This depicts the prograding part of the first order P-R cycle associated with the filling-up of the basin. c) schematic illustration of first, second and higher order P-R cycles in an asymmetric footwall exhumation controlled basin. The purple polygon reflects higher order P-R cycles from the observed progradation from figure 12 & 19.

6. Tectonic and sedimentary evolution of the Konjic Basin in context of the Dinarides

Post-Variscan formations as well as Variscan metasediments and metavolcanics, that are disconformable overlain by rocks of the Alpine cycle and Mesozoic cover (Hrvatovic, 2005), suggest that the Konjic Basin sediments are deposited on the Pre-Karst nappe (fig. 1b). The Cretaceous to Oligocene contraction, which caused the Eocene thrusting of the Pre-Karst nappe over the High-Karst nappe was followed by Early - Middle Miocene extension (see also van Unen et al., 2018). Tapering of alluvial-fluvial packages (figs. 19 and 12), imbrication and cross beds (fig. 11; fig. 13) indicate SW transport of Mid-Bosnian Schist Mountain clasts. This infers that deposition in the Konjic Basin is driven by SW dipping normal faults and MBSMs exhumation at the NE basin margin created the observed asymmetric extensional geometry. The filling-up of the basin follows a first-order retrogradation followed by progradation. The retrogradation is characterized by multiple normal faulting events leading to subsidence and migration of facies basin outward. The basin is subsequently filled-up as fault activity starts to cease covering distal facies with more proximal fluvial and alluvial sediments (figs. 18 and 21).

The Konjic Basin has significant differences when compared with the evolution of other DLS basins in the External Dinarides. These other basins are characterized by asymmetrical basin formation with extensive footwall uplift controlled by detachments in weak zones of the inherited Dinaride nappe contacts, suture zones or orogenic wedges related to the opening of the Pannonian basin (Ilic and Neubauer, 2005; Matenco and Radivojevic, 2012; van Unen et al., 2018). Like the other DLS basins, the Konjic Basin is an asymmetric basin bounded by a normal fault on the NE margin (i.e. Vrbas Fault) that allowed major uplift of the MBSMs in the footwall. Coeval exhumation of the Mid-Bosnian Schist Mountains and deposition in the Konjic Basin is supported by the observation of eroded clasts derived from the same mountains and deposited in the hanging wall of the Vrbas fault system. The Mid-Bosnian Schist Mountains (part of the Pre-Karst nappe), that are exhuming on the NE margin of the Konjic Basin, are bounded by the Buscovača fault in the NE on the SW margin of the Sarajevo-Zenica Basin (fig. 1b; fig. 24). The normal fault system in the Sarajevo-Zenica basin created ~8km of footwall exhumation of this Buscovača fault (Andrić et al., 2017; van Unen et al., 2018). The detachment, formed in the rheological weak Bosnian Flysch (in the Sarajevo-Zenica Basin) is the main cause for the exhumation of the Mid-Bosnian Schist Mountains adjacent to the Konjic Basin (Andrić et al., 2017; van Unen et al., 2018). Here we propose that Mid-Bosnian Schist Mountains exhumation was also controlled by the observed normal fault system in the Konjic Basin. The uplift of the MBSMs is bounded in the SW by the Vrbas fault that is rooted in the thrust between the Pre-Karst and High Karst nappe. This is further emphasized by previously conducted thermochronological studies, which show that the deposition in the Konjic Basin postdate one stage of exhumation of the Mid-Bosnian Schist Mountains by a few million years, before their final exhumation that took place during the post-Middle Miocene inversional event (Casale, 2012; Andrić et al., 2017). This is in agreement with the Middle Miocene extensional deposits dated through flora and mammalian fauna found in coal and clay layers in the adjacent Prozor Basin (Malez and Slišković, 1976). The Sarajevo-Zenica Basin is the furthest previously described vicinity that was affected by the opening of the Pannonian Basin (Ilic and Neubauer, 2005; Matenco and Radivojevic, 2012; Andrić et al., 2017). Although, the development of Konjic Basin is not controlled by formation of a detachment in an inherited weak zone as in other known DLS basins, it is related to the opening of the Pannonian Basin through the causal link with exhumation of the MBSMs and the Sarajevo-Zenica Basin (fig. 24).

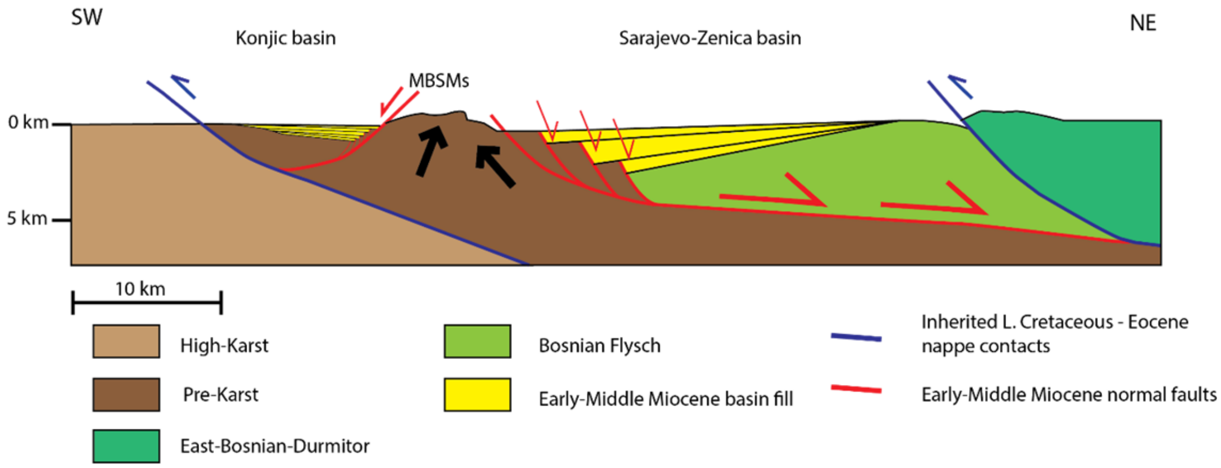

Figure 24: simplified regional transect through the Konjic Basin, Mid-Bosnian Schist Mountains and the Sarajevo-Zenica basin illustrating the relations between inherited thrusts (nappe contacts), Miocene extension, footwall exhumation and basin fill. See text for detailed description of basin formation driving mechanisms. Figure modified after the results from this study and van Unen et al., 2018; Andrić et al., 2017 and this study). See figure 1b for the A-A' transect illustrated in this figure.

Paleoenvironmental studies suggest that the Middle Miocene Climatic Optimum (MCO) (16.9-14.7 Ma, de Leeuw et al., 2011) was one of the key factors in the DLS basin formation and evolution (Mandic et al, 2011) by its enhanced precipitation over evapo-transpiration (Leever et al., 2011). Cyclostratigraphic observations suggest that these DLS basins are highly susceptible to climatic changes, while their preservation s depends on the availability of accommodation space (Mandic et al., 2010; 2011). Our study is consistent with previous studies indicating that the Konjic Basin is mainly tectonically controlled and, in regional context, is in agreement with the regional evolution of the internal Dinarides during the opening of the Pannonian basin ~20 Myr ago.

7. Conclusions

The detailed sedimentological and kinematic analysis in the asymmetric Konjic Basin, a Middle Miocene endemic basin on the SW margin of the internal Dinarides, has revealed a novel extensional mechanism that has not yet been suggested for DLS basins in the Dinarides. Therefore, the results found in this study have inferences for the current view on evolution of the entire Dinarides.

The NE-SW main orientation of the Middle Miocene extension has created the present day geometry of the Konjic Basin and was associated with a phase of peak normal faulting activity followed by reduced normal faults offsets that formed during a waning stage of the basin. Grouping of facies units defined a total of 7 facies associations. The facies associations distinguished prograding and retrograding (P-R) cycles in the sedimentary record. A causal link has been recognized between both faulting phases and the P-R cycles. A distinction can be made between first-order and second-order P-R cycles. Second-order P-R cycles reflect the activity of a set of related normal faults and indicate moments of tectonic activity. The larger, first-order P-R cycles can be subdivided into a retrograding part associated with the high activity of normal faulting, and a prograding part linked to the waning stage of faulting. The first-order retrogradation is linked to a rapid increase in the accommodation space, recognized in the sedimentary record as an overall fining upward trend and basin-ward facies migration. This first order retrogradation is perturbated by slumps and coarser packages associated with moments of fault activity. The first-order progradation is generated by low rates of accommodation space creation, linked to the second extension phase and ongoing sediments supply. It is recognized by its typical overall coarsening upward trend and basin-ward migration of the facies associations. Mid-Bosnian Schist Mountain exhumation is controlled by the detachment, formed in the rheological weak Bosnian Flysch in the Sarajevo-Zenica Basin and the observed SW-dipping normal fault system in the Konjic Basin. Extensive Middle Miocene footwall exhumation of MBSM clasts provided source for the infilling of asymmetric Konjic Basin.

In broader perspective, an asymmetrical, footwall-exhumation controlled basin shows a distinct sedimentary record at times of extensional deformation. This is observed in both the first- and second-order prograding and retrograding cycles. Unidirectional transport of exhumed footwall is often observed in intra-montane basins. Traditionally these basins are dominated by inherited weak zones like nappe contacts. This study, however, presented exhumation of the footwall without a rheological weakness in the basin. Due to the vast amount of DLS basins in the external Dinarides it is suggested that other basins are controlled by the same extensional mechanism. It is advised to study more relatively smaller asymmetric DLS basins nearby larger detachment controlled basins to confirm the mechanism as proposed in this study.

8. Acknowledgements

Thank you for reading this Master Thesis. That is the first acknowledgement to make. I wanted to write a thesis that you enjoyed reading and I enjoyed writing, and I can assure you that the latter was achieved. Wanting to write something and actual putting the words on paper is not the same, but I was very lucky to have the guidance of Prof. Dr. Liviu Matenco and Dr. Nevena Andrić, helping me to narrow down my broad-ranging ideas into a feasible thesis. Liviu is acknowledged for giving me this opportunity, and for his help defining the essence of this thesis. Particular mentions to Nevena for her emails packed with knowledge and comments on my questions. I am grateful for the support I received from BSc. Yola Hesselberth, Prof. dr. Hazim Hrvatovi, MSc. Vedad Demir and Mag. Dr. Oleg Mandic in the field and the pleasant stay Bosnia and Herzegovina provided us with.

9. References

Andrić, Nevena et al. 2017. “The Link between Tectonics and Sedimentatioandircn in Asymmetric Extensional Basins: Inferences from the Study of Sarajevo-Zenica Basin.” Marine and Petroleum Geology 83:305–32.

Andrić, Nevena, Liviu Matenco, Frits Hilgen, and Hans de Bresser. 2018. “Structural Controls on Sedimentation during Asymmetric Extension: The Case of Sorbas Basin (SE Spain).” Global and Planetary Change (November 2017):1–22.

Bouma, Arnold. H. 1964. "Turbudites". Developments in Sedimentology 3: 247-256

Bertotti, G., Y. Podladchikov, and A. Daehler. 2000. “Dynamic Link between the Level of Ductile Crustal Flow and Style of Normal Faulting of Brittle Crust.” Tectonophysics 320(3–4):195–218.

Brun, Jean Pierre and Claudio Faccenna. 2008. “Exhumation of High-Pressure Rocks Driven by Slab Rollback.” Earth and Planetary Science Letters 272(1–2):1–7.

Balázs, A., Matenco, L., Magyar, I., Hortváth,F., Cloetingh, S. 2016. "The link between tectonics and sedimnetation in back-arc basins: new genetic constraints from the analysis of the Pannonian Basin.."Tectonics 35:1526-1559

Breda, A., Melleree, D., Massari, F. 2007. "Facies and processes in a Gilbert-delta-filled incised valley (Pliocene of Ventimiglia, NW Italy)". Sedimentary Geology 200: 31-55

Bryant, M., P. Falk, and C. Paola. 1995. “Experimental Study of Avulsion Frequency and Rate of Deposition.” Geology 23(4):365–68.

Casale, Gabriele M. 2012. “Core Complex Exhumation in Peri-Adriatic Extension, and Kinematics of Neogene Slip along the Saddle Mountains Thrust.”

Catuneanu, Octavian. 2002. “Sequence Stratigraphy of Clastic Systems: Concepts, Merits, and Pitfalls.” Journal of African Earth Sciences 35(1):1–43.

DeCelles, P. G. et al. 1991. “Controls on Synorogenic Alluvial-fan Architecture, Beartooth Conglomerate (Palaeocene), Wyoming and Montana.” Sedimentology 38(4):567–90.

García-García, Fernando, Juan Fernández, César Viseras, and Jesús M. Soria. 2006. “Architecture and Sedimentary Facies Evolution in a Delta Stack Controlled by Fault Growth (Betic Cordillera, Southern Spain, Late Tortonian).” Sedimentary Geology 185(1–2):79–92.

Gawthorpe, R. L. and A. Colella. 2009. “Tectonic Controls on Coarse-Grained Delta Depositional Systems in Rift Basins.” Coarse-Grained Deltas 113–27.

Harzhauser, Mathias and Oleg Mandic. 2008. “Neogene Lake Systems of Central and South-Eastern Europe: Faunal Diversity, Gradients and Interrelations.” Palaeogeography, Palaeoclimatology, Palaeoecology 260(3–4):417–34.

Hesselberth, Y. 2018. "Understanding the kinematic evolution of asymmetric extensional basins during the Miocene evolution of the Dinarides

Horváth, F. et al. 2015. “Evolution of the Pannonian Basin and Its Geothermal Resources.” Geothermics 53:328–52.

Hrvatovic, Hazim, 2005. "Geological Guidebook Trough Bosnia and Herzegovina". Goological Survey of Federation Bosnai and Herzegovina

Hrvatovic, 2006"Geological Guidebook Trough Bosnia and Herzegovina". Goological Survey of

Federation Bosnai and Herzegovina

Ilić, Aleksandar and Franz Neubauer. 2005. “Tertiary to Recent Oblique Convergence and Wrenching of the Central Dinarides: Constraints from a Palaeostress Study.” Tectonophysics 410(1–4):465–84.

Jolivet, L. and C. Faccenna. 2000. “Mediterranean Extension and the Africa-Eurasia Collision.” Tectonics 19(6):1095–1106.

Korbar, Tvrtko. 2009. “Orogenic Evolution of the External Dinarides in the NE Adriatic Region: A Model Constrained by Tectonostratigraphy of Upper Cretaceous to Paleogene Carbonates.” Earth-Science Reviews 96(4):296–312. Retrieved

De Leeuw, A. 2011. Paleomagnetic and Geochronologic Constraints on the Miocene Evolution of Semi-Isolated Basins in Southeastern Europe.

Leever, K. A., L. Matenco, D. Garcia-Castellanos, and S. A. P. L. Cloetingh. 2011. “The Evolution of the Danube Gateway between Central and Eastern Paratethys (SE Europe): Insight from Numerical Modelling of the Causes and Effects of Connectivity between Basins and Its Expression in the Sedimentary Record.” Tectonophysics 502(1–2):175–95.

Leppard, Christopher W. and Rob L. Gawthorpe. 2006. “Sedimentology of Rift Climax Deep Water Systems; Lower Rudeis Formation, Hammam Faraun Fault Block, Suez Rift, Egypt.” Sedimentary Geology 191(1–2):67–87.

Malez M., Slišković T. 1976. "Starost Nekig naslaga ugljena ugljena u tercijaru Bosne i Hercegovine na osnovi nalaza vertebrata". Geološki glasnik 21, Sarajevo.

Mandic, O., de Leeuw, A., Vukovic,B., Krijgsman, W., Harzhauser, M., Kuiper, K.F., 2011. "Paleoenvironmental evolution of lake Gacko (Southern Bosnia and Herzegovina): impact of the middle Miocene climatic Optimum on the Dinaride Lakes System." Palaeogeography. Palaeoclimatology. Palaeocol. 299:475-492

Matenco, L. and D. Radivojevic. 2012. “On the Formation and Evolution of the Pannonian Basin: Constraints Derived from the Structure of the Junction Area between the Carpathians and Dinarides.” Tectonics 31(6):1–31.

McConnico, T.S. & Bassett, Kari, N. 2007. “Gravelly Gilbert-type fan delat on the Conway Coast, New Zealand: Foreset depositional processes and clast imbrications.” Sedimentary Geology 198: 147-166

Melchor, Ricardo Néstor. 2007. “Changing Lake Dynamics and Sequence Stratigraphy of Synrift Lacustrine Strata in a Half-Graben: An Example from the Triassic Ischigualasto-Villa Unión Basin, Argentina.” Sedimentology 54(6):1417–46.

Pamić, Tomljenović, & Balen, 2002)Pamić, J., Gušic, I., & Jelaska, V. (1998). Geodynamic evolution of the Central Dinarides. Tectonophysics, 297, 251–268.

Pamić, J., Tomljenović, B., & Balen, D. (2002). Geodynamic and petrogenetic evolution of Alpine ophiolites from the central and NW Dinarides: An overview. Lithos, 65(1–2), 113–142.

Pamić, J. et al. 2004. “K-Ar and Ar-Ar Dating of the Palaeozoic Metamorphic Complex from the Mid-Bosnian Schist Mts., Central Dinarides, Bosnia and Hercegovina.” Mineralogy and Petrology 82(1–2):65–79.

Postma, G., Nemec, W., Kleinspehn, K.L. 1988. "Large floating clasts in turbidites: a mechanism for their emplacement." Sedimentary Geology, 58: 47-61

Sant, K., Andrić, N., Mandic, O., Demir, V., Pavelić, D., Rundić, Lj., Hrvatović, H., Matenco, L., Krijgsman, W. 2018. " Magnetostratigraphy and depositional environments of the Miocene freshwater sediments of the Sarajevo-Zenica basin" to be submitted to *Paleo3.*

Schmid, Stefan M. et al. 2008. “The Alpine-Carpathian-Dinaridic Orogenic System: Correlation and Evolution of Tectonic Units.” Swiss Journal of Geosciences 101(1):139–83.

Scholz, C. A., B. R. Rosendahl, and D. L. Scott. 1990. “Development of Coarse Grained-Facies in Lacustrine Rift Basins: Example from East Africa.” Geology 18(February):140–44.

Živanović, M. and Sofilj, Milojević R. 1975. "Basic geological map of SFRY, sheet Zenica !:100.000". Federal geological survey, Belgrade

Støren, Eivind N., Svein Olaf Dahl, Atle Nesje, and Øyvind Paasche. 2010. “Identifying the Sedimentary Imprint of High-Frequency Holocene River Floods in Lake Sediments: Development and Application of a New Method.” Quaternary Science Reviews 29(23–24):3021–33.

Talling, Peter J., Douglas G. M. Masson, Esther J. Sumner, and Giuseppe Malgesini. 2012. “Subaqueous Sediment Density Flows : Depositional Processes and Deposit Types.” Sedimentology 59:1937–2003.

Tomljenović, Bruno and László Csontos. 2001. “Neogene-Quaternary Structures in the Border Zone between Alps, Dinarides and Pannonian Basin (Hrvatsko Zgorje and Karlovac Basins, Croatia).” International Journal of Earth Sciences 90(3):560–78.

van Unen, Marianne et al. 2018. “Kinematics of Foreland-Vergent Crustal Accretion : Inferences from the Dinarides Evolution.” Tectonics (Submitted) 1–50.

Ustaszewski, Kamil, Marijan Herak, Bruno Tomljenović, Davorka Herak, and Srebrenka Matej. 2014. “Neotectonics of the Dinarides-Pannonian Basin Transition and Possible Earthquake Sources in the Banja Luka Epicentral Area.” Journal of Geodynamics 82:52–68.

Appendix A

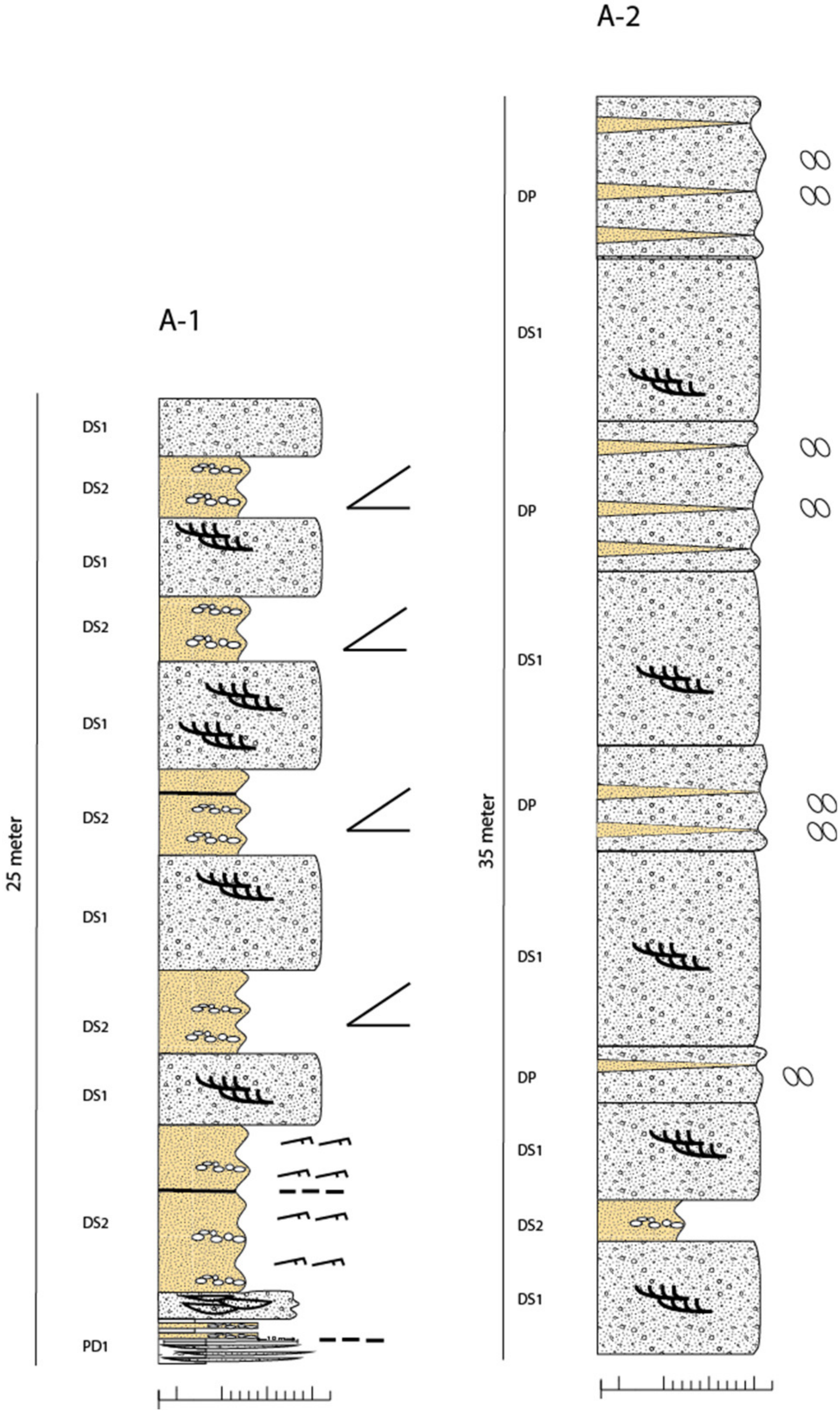

Appendix A-1 and A-2

A-3

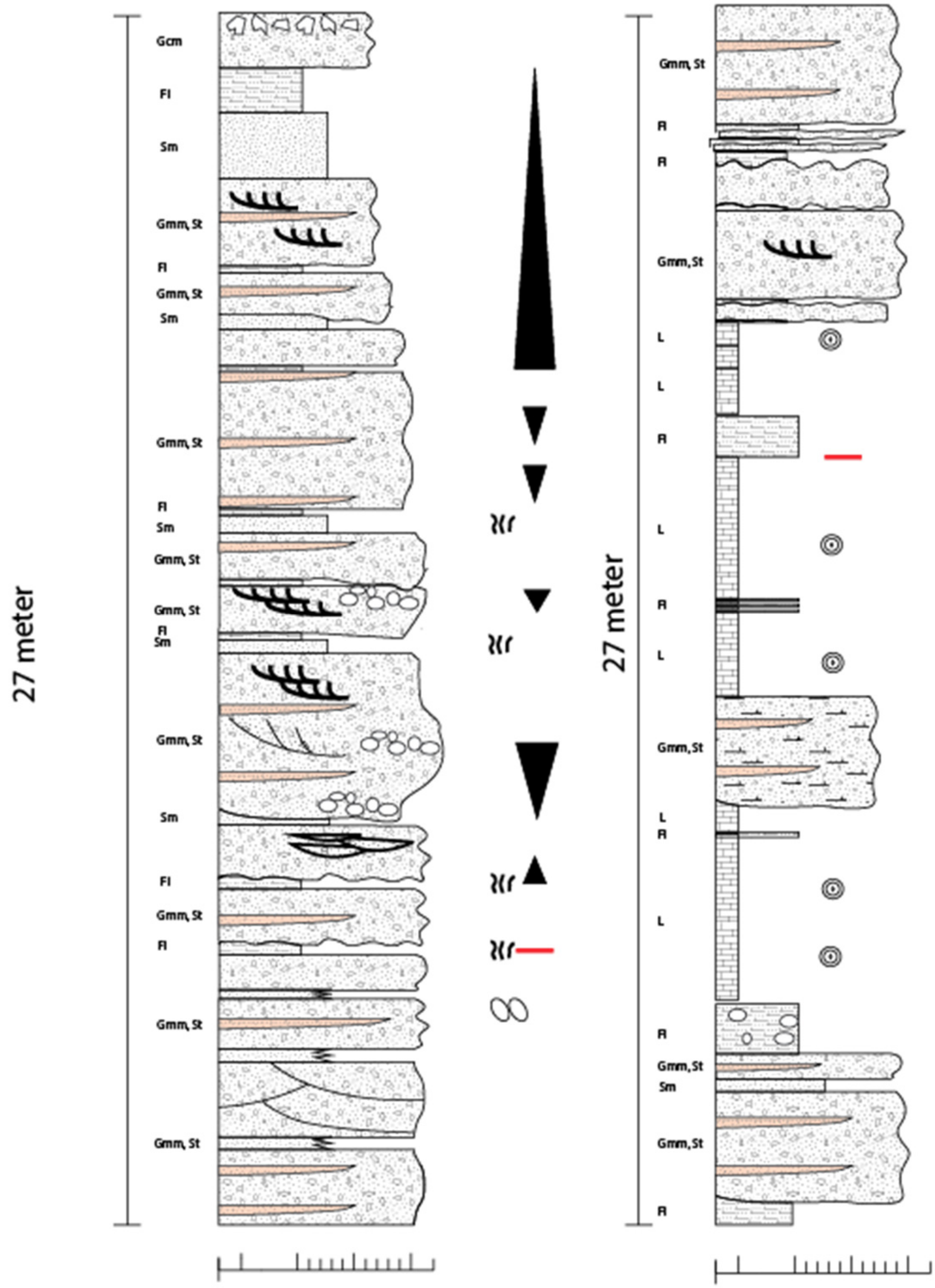

Appendix A-3

A-4

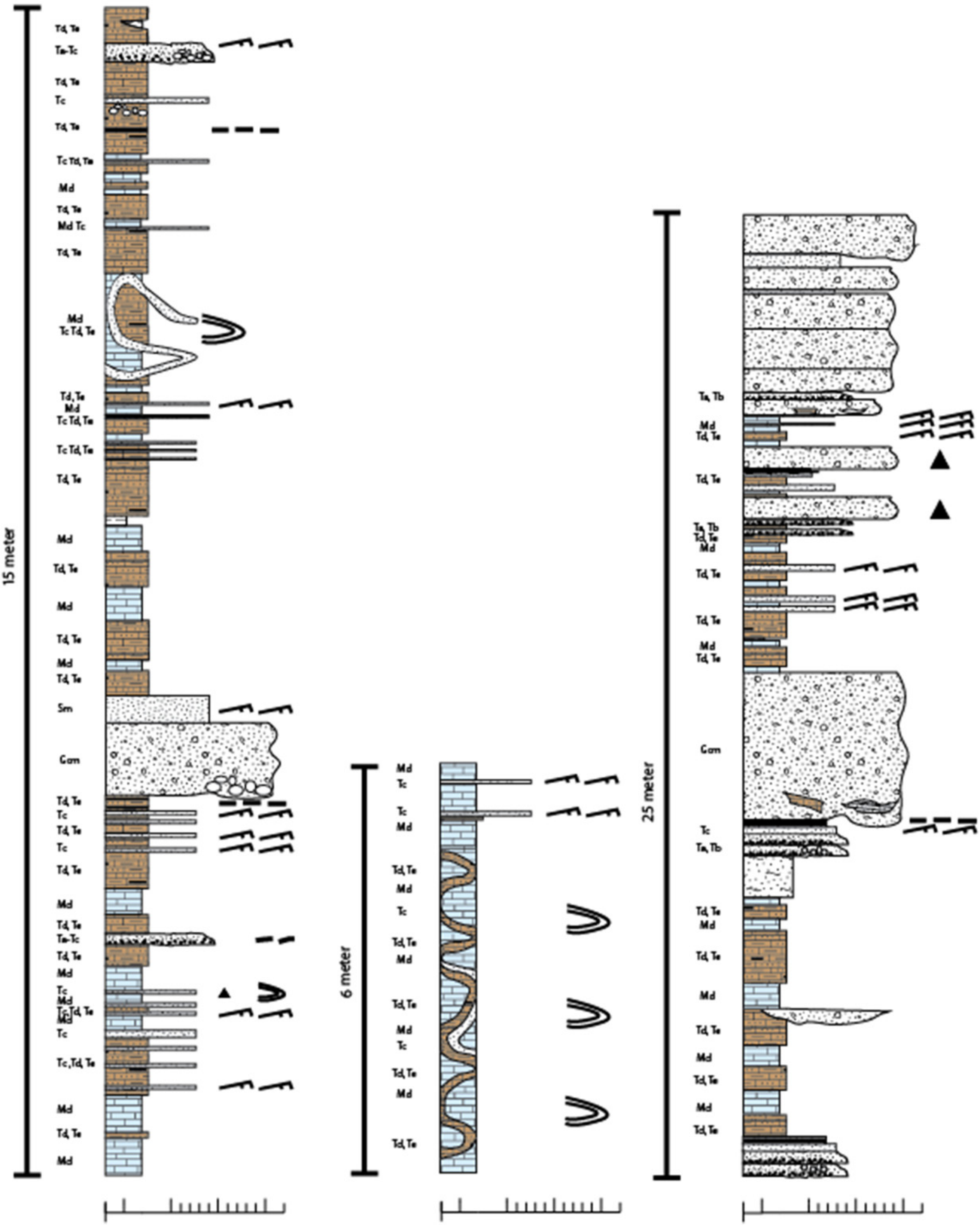

Appendix A-4

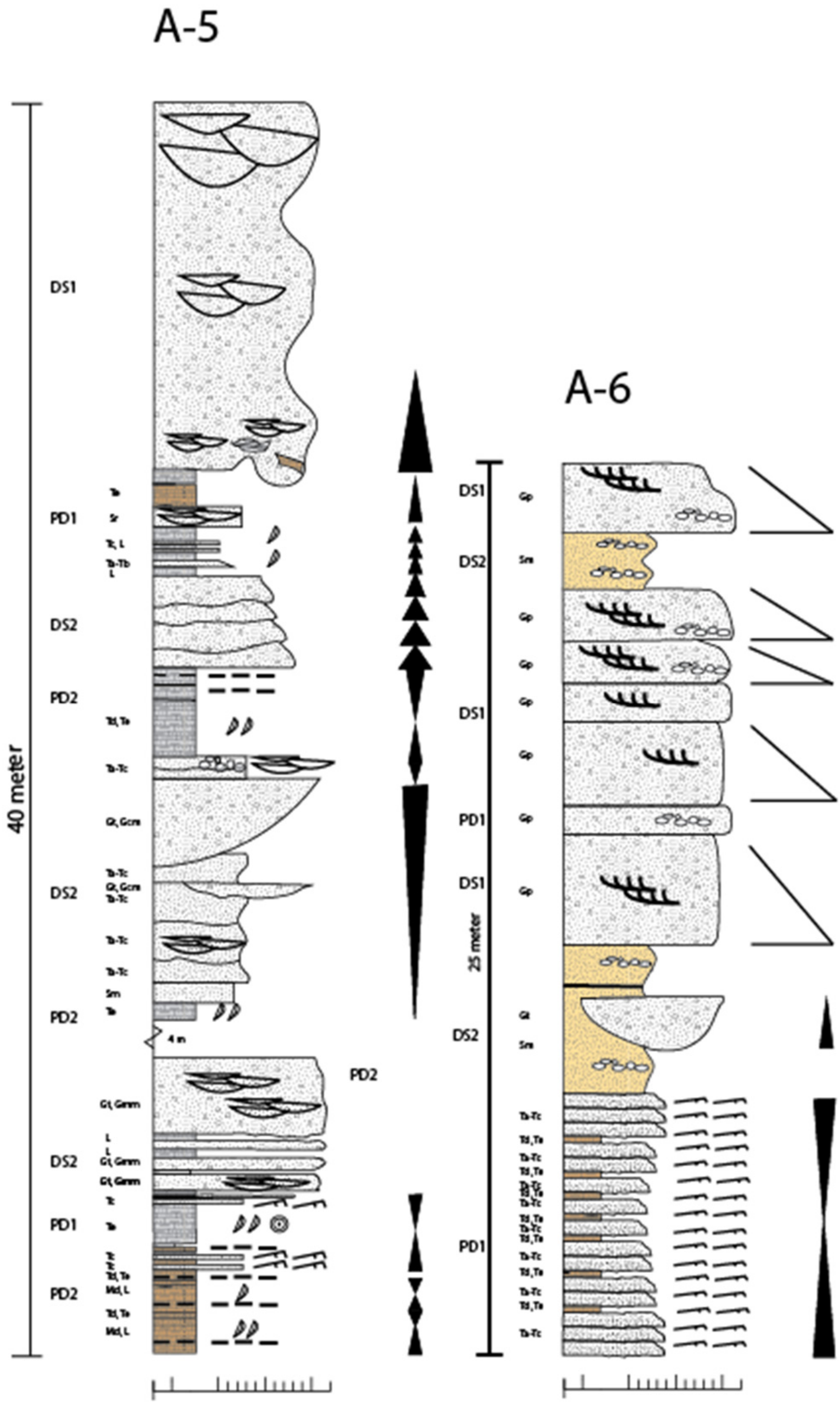

Appendix A-5 and A-6